

**NASA
Technical
Memorandum**

NASA TM- 100395

**DEFINITION OF LARGE COMPONENTS ASSEMBLED
ON-ORBIT AND ROBOT COMPATIBLE MECHANICAL JOINTS**

By J. Williamsen, F. Thomas, J. Finckenor, and B. Spiegel

Structures and Dynamics Laboratory
Science and Engineering Directorate

April 1990

(NASA-TM-100395) DEFINITION OF LARGE
COMPONENTS ASSEMBLED ON-ORBIT AND ROBOT
COMPATIBLE MECHANICAL JOINTS (NASA) 43 p
CSCL 13T

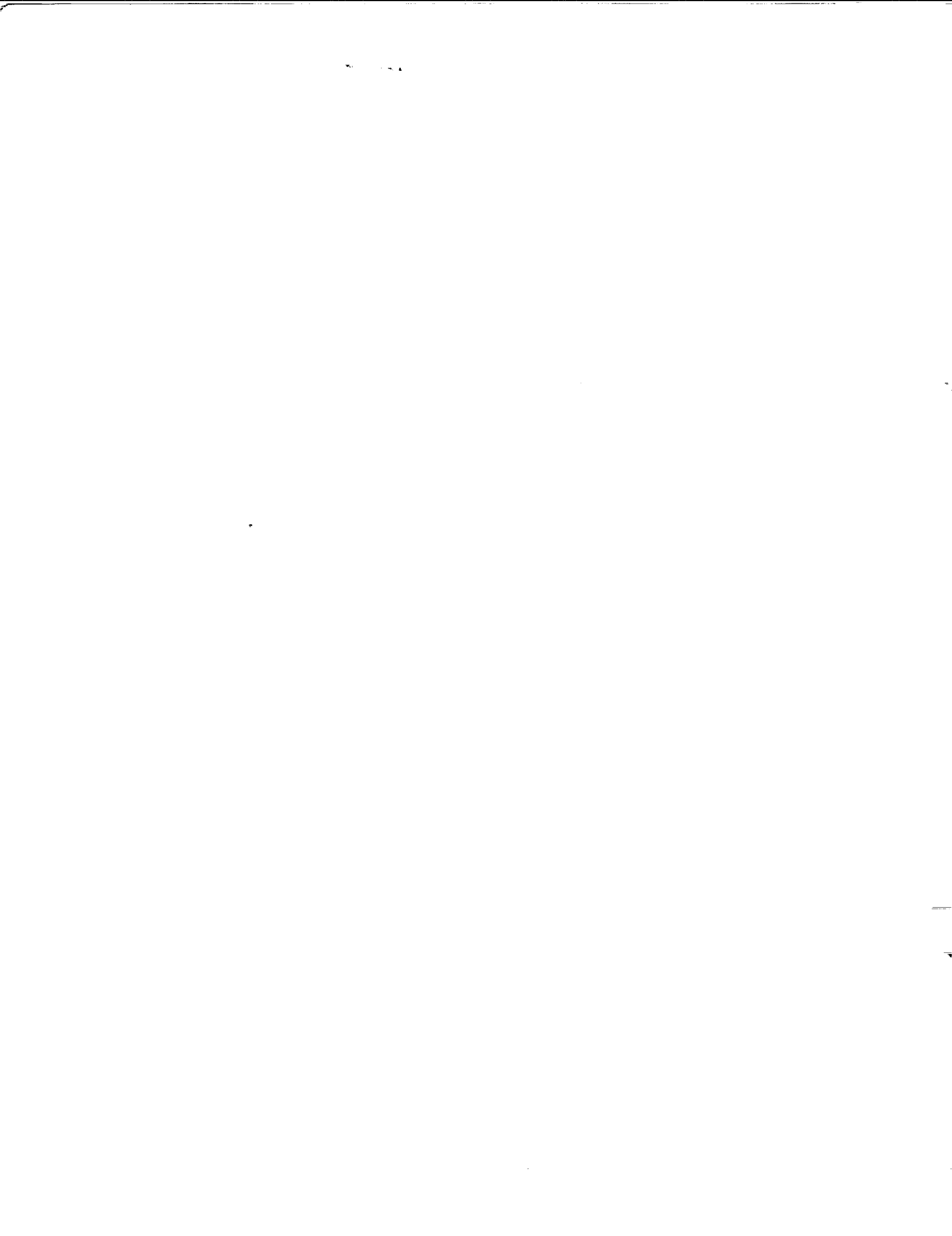
N90-22043

Unclas
G3/37 0279341



National Aeronautics and
Space Administration

George C. Marshall Space Flight Center





Report Documentation Page

1. Report No. NASA TM-100395		2. Government Accession No.		3. Recipient's Catalog No.	
4. Title and Subtitle Definition of Large Components Assembled On-Orbit and Robot Compatible Mechanical Joints				5. Report Date April 1990	
				6. Performing Organization Code	
7. Author(s) J. Williamsen, F. Thomas, J. Finckenor, and B. Spiegel				8. Performing Organization Report No.	
				10. Work Unit No.	
9. Performing Organization Name and Address George C. Marshall Space Flight Center Marshall Space Flight Center, Alabama 35812				11. Contract or Grant No.	
				13. Type of Report and Period Covered Technical Memorandum	
12. Sponsoring Agency Name and Address National Aeronautics and Space Administration Washington, D.C. 20546				14. Sponsoring Agency Code	
15. Supplementary Notes Prepared by Structures and Dynamics Laboratory, Science and Engineering Directorate.					
16. Abstract <p>One of four major areas of project Pathfinder is in-space assembly and construction. The task of in-space assembly and construction is to develop the requirements and the technology needed to build elements in space.</p> <p>This paper identifies a 120-ft diameter tetrahedral aerobrake truss as the focus element. A heavily loaded mechanical joint is designed to robotically assemble the defined aerobrake element. Also, typical large components such as habitation modules, storage tanks, etc., are defined, and attachment concepts of these components to the tetrahedral truss are developed.</p>					
17. Key Words (Suggested by Author(s)) Mechanical Joints In-Space Assembly Large Components			18. Distribution Statement Unclassified/Unlimited		
19. Security Classif. (of this report) Unclassified		20. Security Classif. (of this page) Unclassified		21. No. of pages 42	22. Price NTIS



TABLE OF CONTENTS

	Page
I. INTRODUCTION	1
II. AEROBRAKE STUDIES	1
III. TRANSITION TRUSS	11
IV. LARGE COMPONENTS	16
V. MECHANICAL JOINTS	20
VI. CONCLUSION	25
REFERENCES	29
BIBLIOGRAPHY	29
APPENDIX A—STRESS ANALYSIS	30

LIST OF FIGURES

Figure	Title	Page
1.	Vehicle definition study	3
2.	Pathfinder aerobrake configuration	4
3.	Aerobrake truss element loading definition	5
4.	Aerobrake truss element loading definition detail.....	6
5.	Four-point payload constraint.....	7
6.	Eight-point payload constraint.....	8
7.	Axial load versus element number, four-point payload constraint.....	9
8.	Axial load versus element number, eight-point payload constraint.....	10
9.	Variation of axial load	12
10.	Transition truss – aerobrake support structure.....	13
11.	Transition truss – spherical components.....	14
12.	Transition truss – cylindrical components.....	15
13.	Threaded screw joint	21
14.	Threaded screw joint mating sequence	22
15.	Grip joint configuration.....	23
16.	Grip joint	24
17.	Clevis joint mating sequence.....	26
18.	Slip joint	27

LIST OF TABLES

Table	Title	Page
1.	Large components required for Earth departure	17
2.	Large components required for Earth return from Mars	18
3.	Large components thermal and radiation protection	19



TECHNICAL MEMORANDUM

DEFINITION OF LARGE COMPONENTS ASSEMBLED ON-ORBIT AND ROBOT COMPATIBLE MECHANICAL JOINTS

I. INTRODUCTION

The Pathfinder Project was conceived to develop the technology required for future space flight missions, such as establishing a permanent presence on the Moon, a manned mission to Mars, or a combination of both. There are four key areas to Project Pathfinder: in-space assembly and construction, extraplanetary exploration (including remote surveillance and surface exploration, humans-in-space (including closed-loop life support and space medical science), and transfer vehicle technology (providing the means for leaving and returning to low Earth orbit).

The Pathfinder in-space assembly and construction activity focuses on the technology that is needed to construct large, massive, and complex vehicles in space. The program is intended to provide a wide range of design options that are independent of any particular vehicle or platform concept. There are four main objectives for this task:

1. Define methodologies for constructing generic spacecraft components, such as aerobrake shells, backbone trusses, and pressurized modules, that can be applied to a variety of different missions.
2. Develop processes for joining components in space, including welding, bonding, and mechanical fastening.
3. Develop the ability to manipulate and precisely position elements and large components so that they can be joined.
4. Define the facility layout and infrastructure that would be required to support the construction of entire large space vehicles and platforms in orbit.

NASA/Marshall Space Flight Center (MSFC) is responsible for defining generic large spacecraft components and the methods for building them on orbit, including welding and mechanical joining processes. The primary purpose of this report is to document (1) the definition of some "typical" large components in space, and (2) the development of joint load requirements and concepts for use in assembly of large space components.

II. AEROBRAKE STUDIES

The Structures Division at MSFC had previously performed several studies to further define "typical" configurations, loads, and packing requirements for aerobraked vehicles. This work was

done primarily to support mechanical joint detailed design for in-space assembly and construction. During this early work, a search for mission studies utilizing aerobraked vehicle concepts was performed. The studies of greatest interest and value are listed in the bibliography.

Through analysis of these reports and discussions with Langley Research Center (LaRC), the "generic" vehicle concept shown in Figure 1 emerged as the baseline for the studies. As can be seen, this vehicle concept is based upon a 120-ft (36.57-m) diameter aerobrake with a spherical surface. This aerobrake would be assembled on-orbit using hexagonally shaped thermal panels attached to a tetrahedral truss structure. Large components would be attached to the back side of the aerobrake truss through an intermediate or "transition" truss (see Section III, Transition Truss, and Section IV, Large Components). Figure 2 shows a detail of the baselined aerobrake structural assembly. The concept, while not intended to represent an optimized design, did make possible a derivation of first-order requirements for heavily loaded structural joints which were used in the MSFC detailed design efforts (see Section V, Mechanical Joints).

A finite element model of the baseline aerobrake structure was then developed in order to identify loads at mechanical joints within the aerobrake truss using MSC Pal, a personal computer version of NASTRAN. For the purpose of this model, the spherical aerobrake profile was approximated as flat, as shown in Figure 3. Figure 4 outlines further assumptions made in the configuration and exterior loading of the aerobrake model. The hexagon size chosen for the thermal panels was 14.5 ft (4.42 m) from corner to corner, the maximum size that could be stacked within the space transportation system orbiter bay. From this, the total number of thermal panels for the aerobrake was derived as 61, yielding a total aerobrake area of 8,330 ft² (773.88 m²). The length of each of the aerobrake struts, 12.55 ft (3.83 m) from node center to node center, was also derived from the size assumed for the aerobrake panels (with three struts forming the equilateral triangular support base for each aerobrake panel). The thickness of the overall aerobrake structure, 10.25 ft (3.12 m), results from the geometry of placing struts of this size within a tetrahedral arrangement. It is important to note that a spherical aerobrake profile would result in a number of different sizes of struts within the aerobrake truss (rather than the one size determined for the flat truss) with an accompanying increase in assembly complexity.

The point loads applied to all of the "front" aerobrake truss nodes (facing the "windstream" during aerobraking) were derived from the vehicle mass and decelerations quoted in Reference 1, as pictured in Figure 4. While these loads were applied to the "front" of the aerobrake, the model was constrained from motion at the "rear" of the aerobrake truss in three different constraint cases, modeling three different payload attachment conditions. Case 1 was a four-point "payload" constraint of model motion at the nodes shown in Figure 5. Case 2 was an eight-point "payload" constraint of model motion at the nodes shown in Figure 6. Case 3 was a multipoint constraint of all model nodes in the lower half of the aerobrake model.

The results from constraint Cases 1 through 3 are shown in Figures 7 through 9. Figure 7 shows that for the four-point payload constraint (Case 1), maximum loads in the truss members varied from +200,000 lb (887.6 kN) to -120,000 lb (-533.76 kN) with the largest loads concentrating in the members around the four nodes of constraint. Figure 8 shows that for the eight-point payload constraint (Case 2) maximum loads in the truss members were lower, varying from +240,000 lb (1,067.52 kN) to -140,000 lb (-622.72 kN) with the largest loads concentrating in the members around the eight nodes of constraint. Case 3, the multipoint payload constraint,

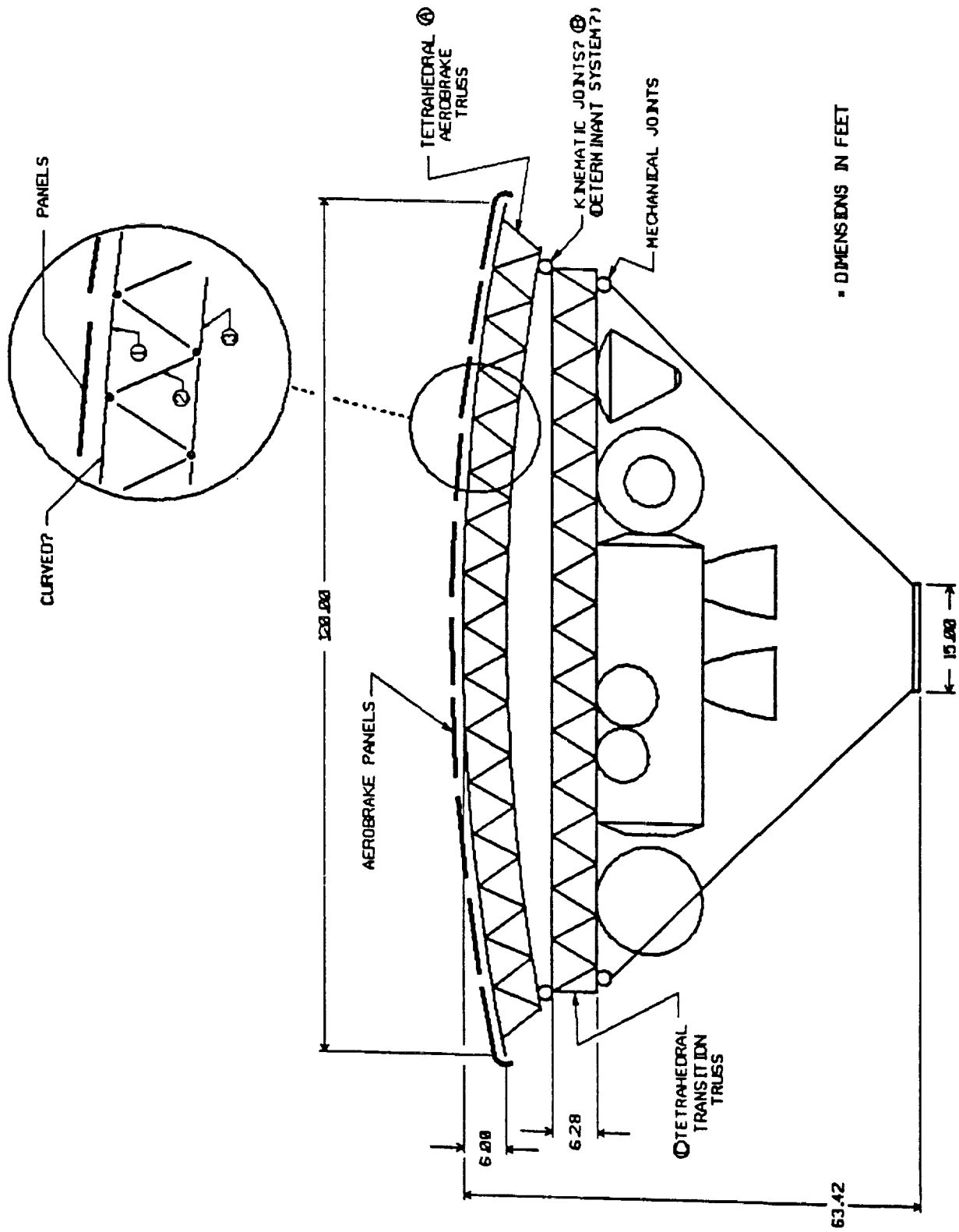


Figure 1. Vehicle definition study.

- 1. COMPONENT
- 2. TRUNNION
- 3. TRANSITION NODE
- 4. TRANSITION TRUSS JOINT
- 5. TRANSITION STRUT
- 6. UPPER AEROBRAKE NODE
- 7. AEROBRAKE TRUSS JOINT
- 8. AEROBRAKE STRUT
- 9. LOWER AEROBRAKE NODE
- 10. PANEL TO AEROBRAKE NODE JOINT
- 11. PANEL TO PANEL JOINT
- 12. AEROBRAKE PANEL

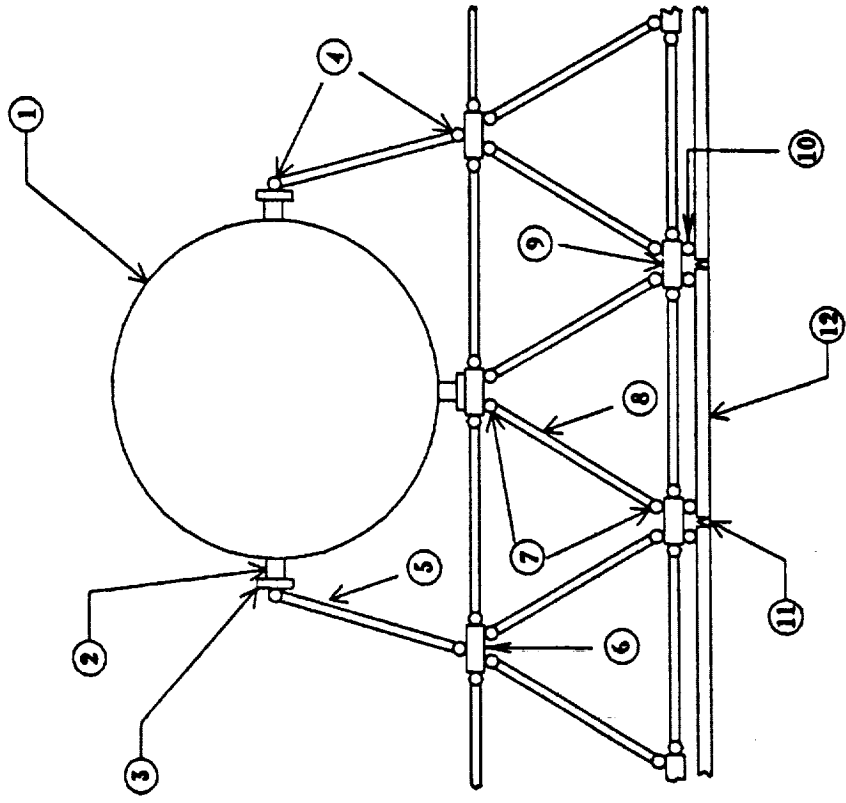


Figure 2. Pathfinder aerobrake configuration.

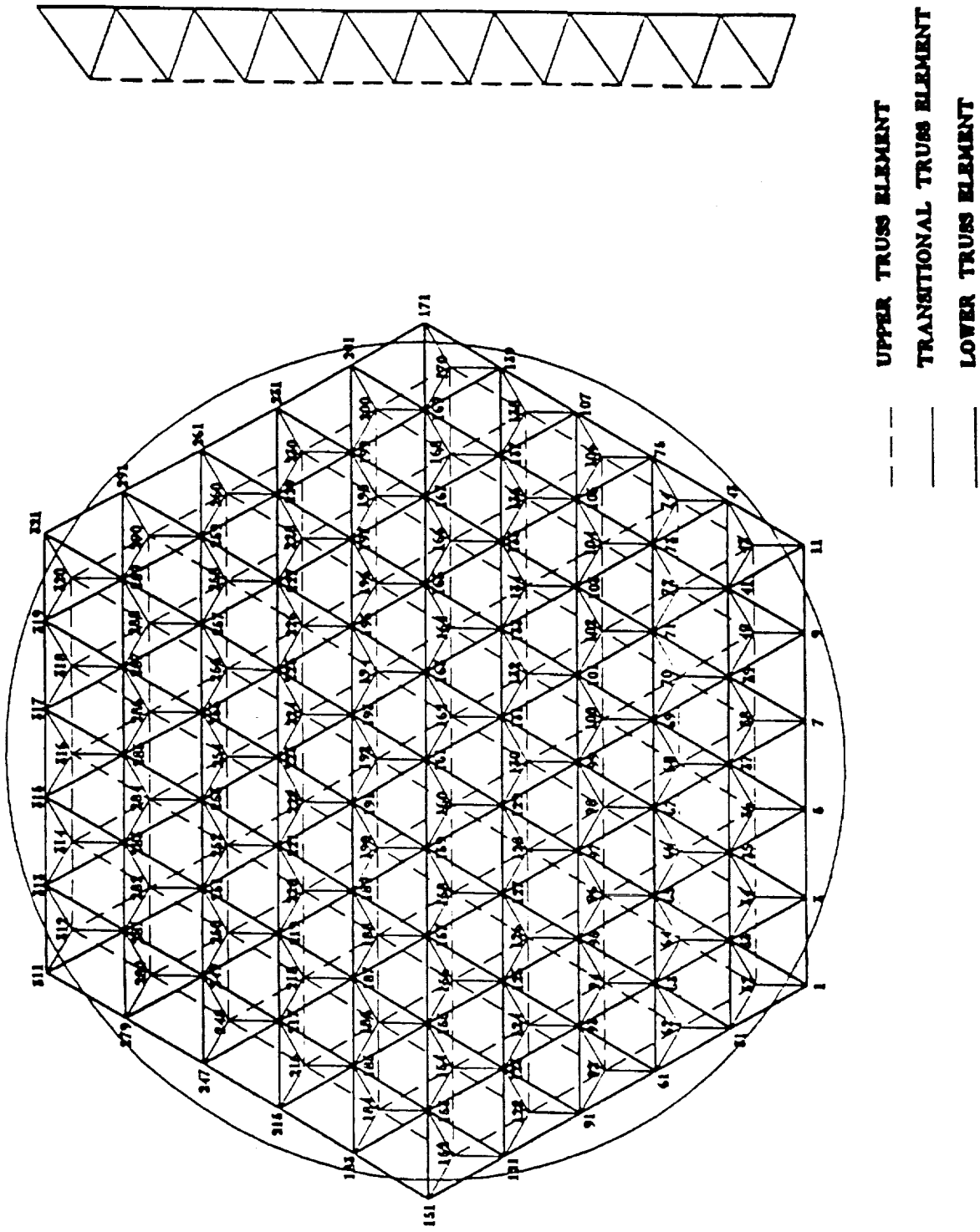


Figure 3. Aerobrake truss element loading definition.

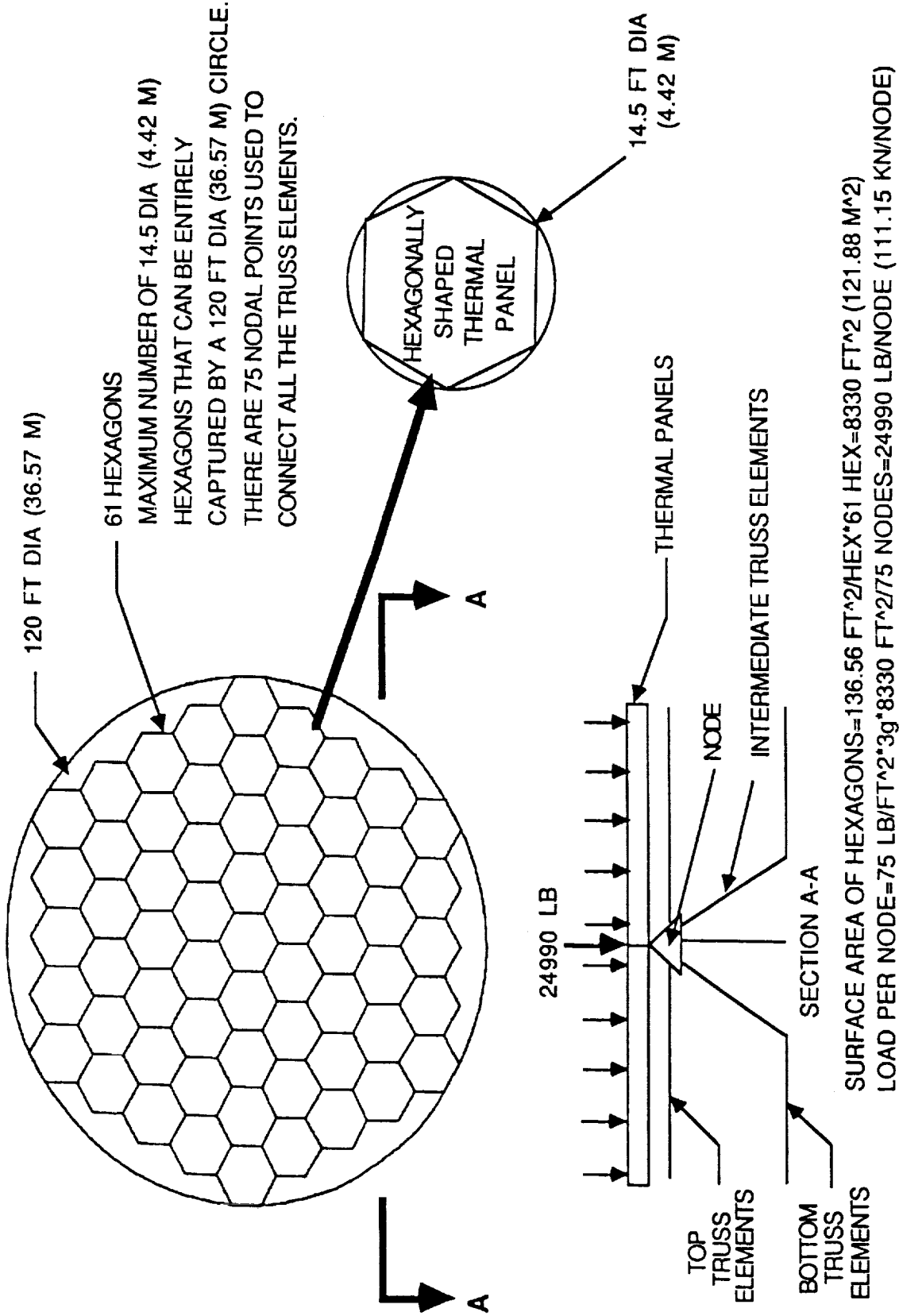


Figure 4. Aerobrake truss element loading definition detail.

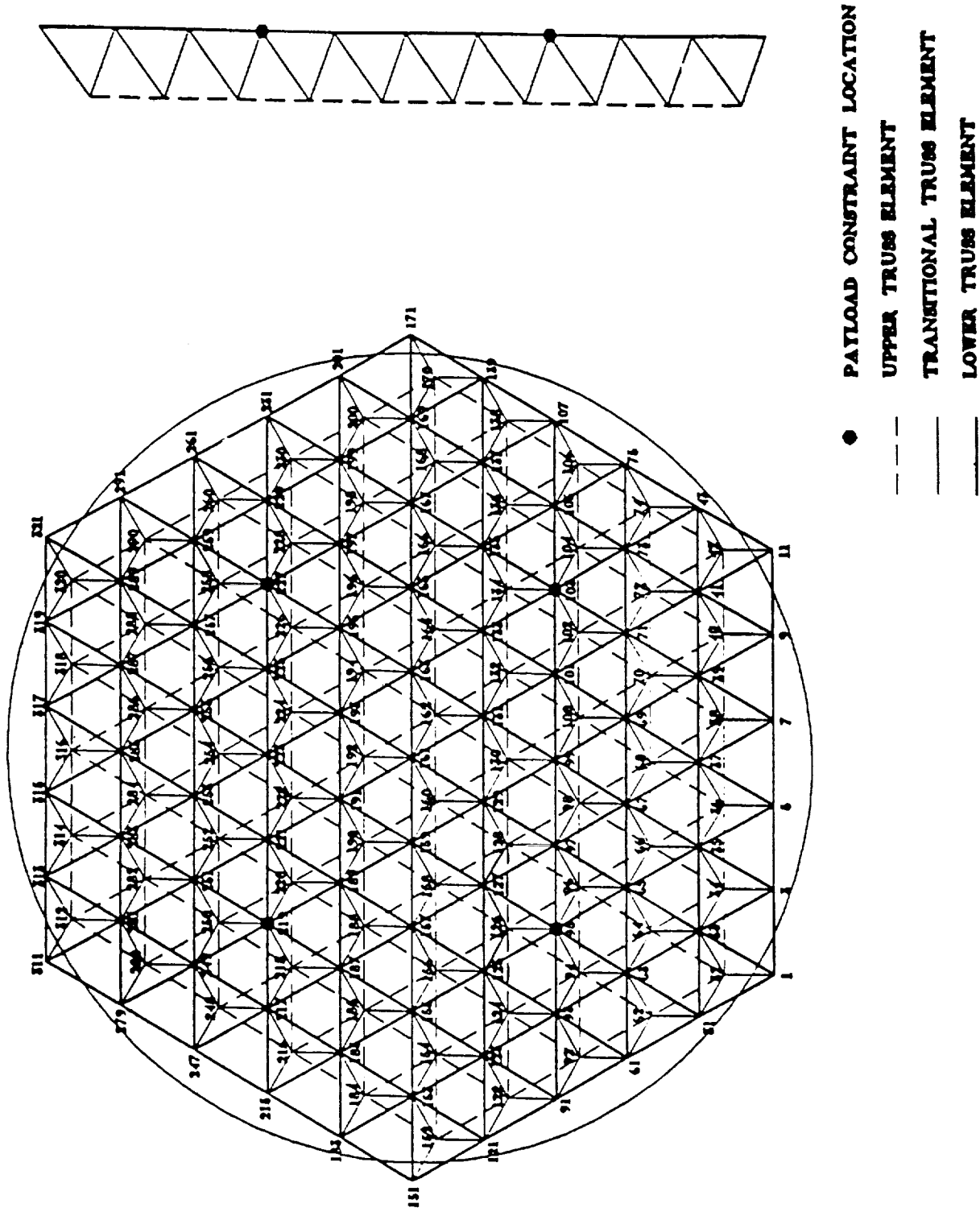
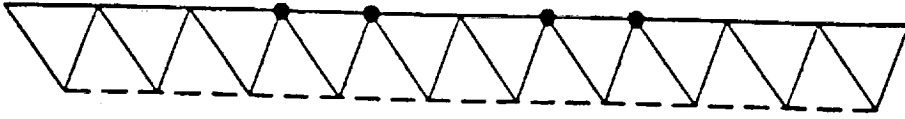
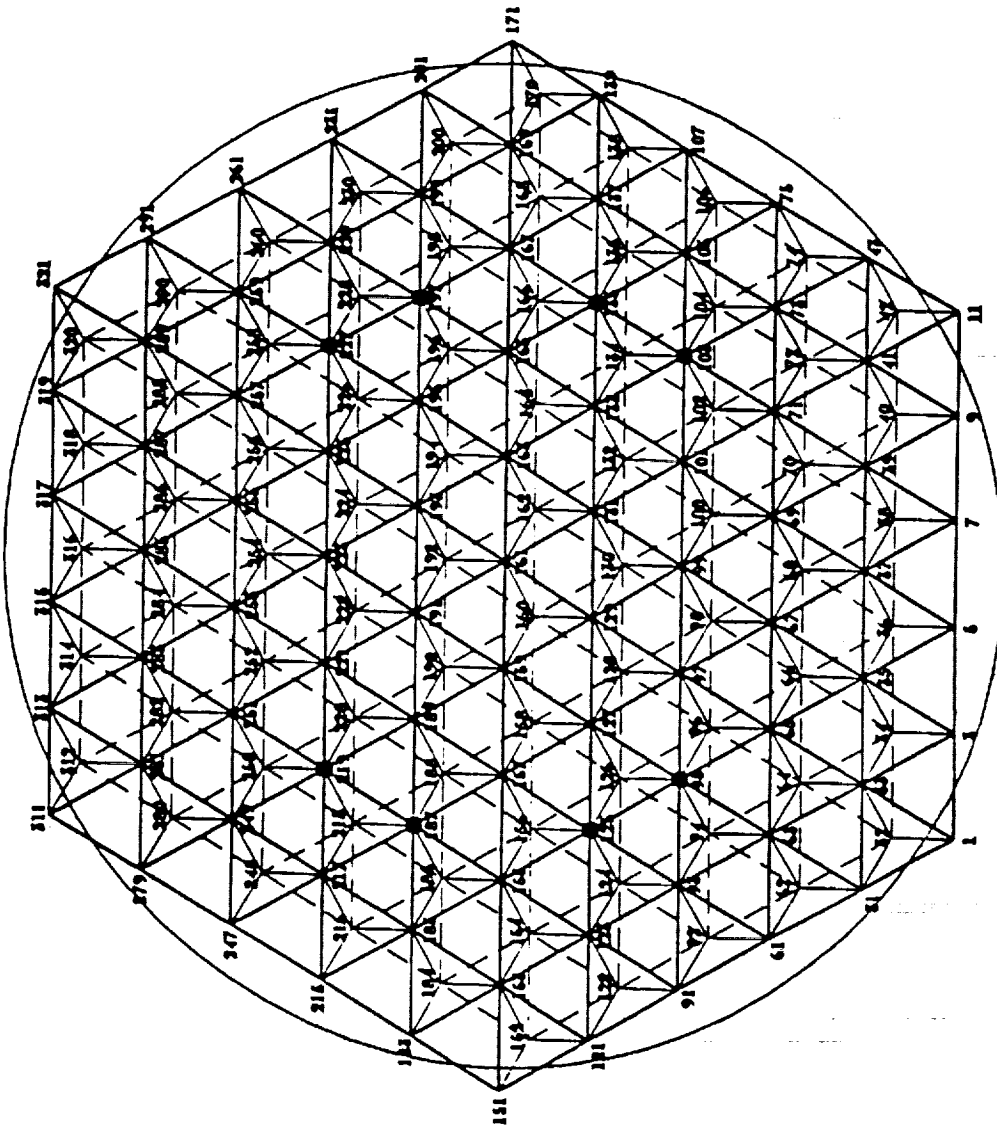


Figure 5. Four-point payload constraint.



- PAYLOAD CONSTRAINT LOCATION
- UPPER TRUSS ELEMENT
- TRANSITIONAL TRUSS ELEMENT
- LOWER TRUSS ELEMENT

Figure 6. Eight-point payload constraint.

ORIGINAL PAGE IS
OF POOR QUALITY

4 PAYLOAD CONSTRAINTS

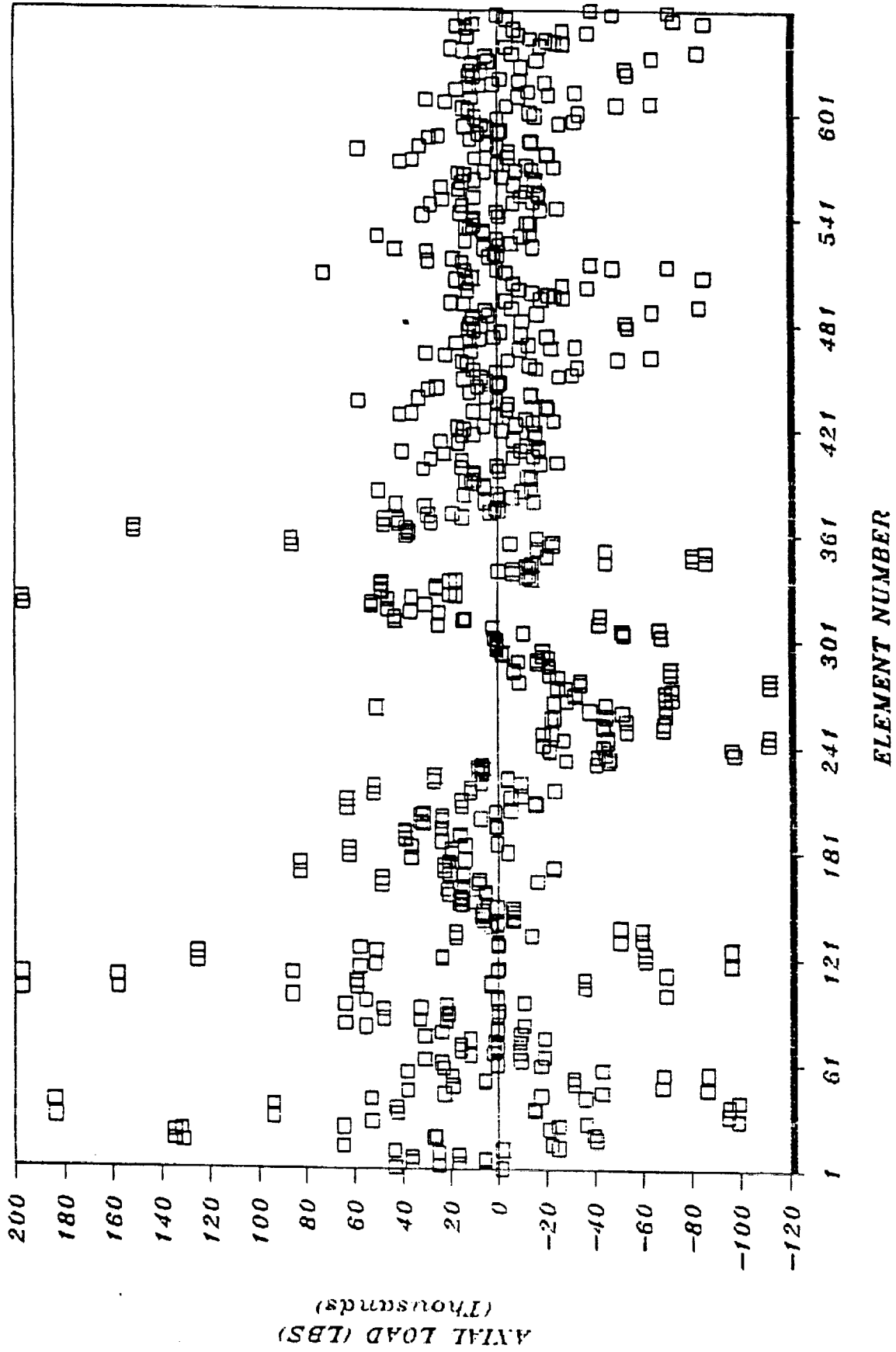


Figure 7. Axial load versus element number, four-point payload constraint.

8 PAYLOAD CONSTRAINTS

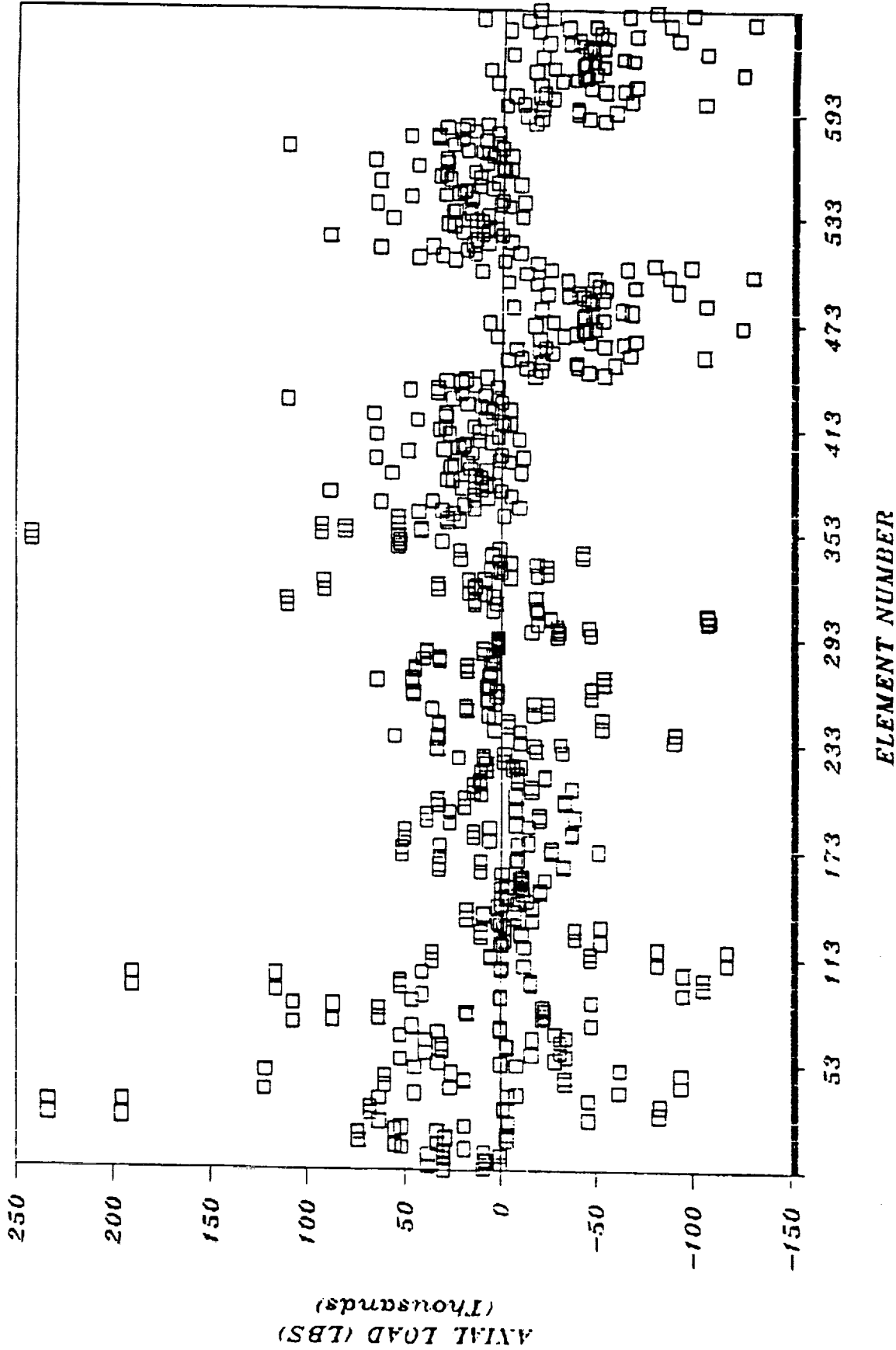


Figure 8. Axial load versus element number, eight-point payload constraint.

showed a roughly equal load in all aerobrake truss members of 13,000 lb (57.82 kN). Loadings for all three cases are broken down by percentages into several ranges and are shown in Figure 9. It was noted that most of the truss member loads (>90 percent) were below 100,000 lb (444.80 kN) in magnitude, even for the worst case constraint (Case 1). This finding, combined with the reasoning that more than eight points of payload connection were probable in the case of a "real" aerobrake, led to the establishment of a 100,000-lb (444.8 kN) load as the preliminary load criteria for mechanical joint design (see Section V, Mechanical Joints).

III. TRANSITION TRUSS

The purpose of the transition truss task was to develop concepts and requirements for attaching large components to an aerobrake truss. A transition truss is defined as the arrangement of structural members that support and connect large components to an aerobrake truss. The components selected for attachment to the aerobrake were typical large and heavy components representative of the data in Section IV, Large Components. The aerobrake configuration for this study was a 120-ft (36.57-m) diameter tetrahedral truss as described in the Aerobrake Study. The plane view of the tetrahedral truss, upon which large components would be attached, is shown in Figure 10. Two types of large components were used to characterize typical transition truss configurations—a 12.91-ft (3.94-m) diameter spherical, liquid oxygen (LOX) tank, and a 42-ft (12.80-m) long by 14.5-ft (4.42-m) diameter Space Station Freedom laboratory module. Figure 11 shows the 12.91-ft (3.94-m) LOX tank and how it is mounted and restrained on the aerobrake. The tank is arranged, and the transition truss structure designed, so that it would easily attach to the aerobrake truss. The LOX tank is connected to the aerobrake truss by six transition truss members at 60-degree locations that correspond to six node locations on the aerobrake truss. Diagonal members are placed between alternating transition truss members to provide for torsional stiffness.

Figure 12 shows the Space Station Freedom laboratory module and how it might be mounted and restrained to the aerobrake truss. The module is arranged, and the transition truss structure designed, so that it would easily attach to the aerobrake truss. The module is connected to the aerobrake truss with four transition truss members and at one keel location, similar to its structural attachment to the space transportation system (STS) cargo bay. The keel attachment is made at the front of the cylinder to an aerobrake truss node.

Preliminary axial loads were determined by building a three-dimensional finite element model of a 12.91-ft (3.94-m) 80,356-lb (357.42-kN) sphere and a 42-ft (12.80-m) long by 14.5-ft (4.42-m) diameter 64,328-lb (286.13-kN) cylinder. The transition truss members were attached to the components and attached to the appropriate location on the aerobrake. The aerobrake, for this analysis, was assumed to be infinitely rigid. The aerobrake node end of the transition truss members was restrained in various configurations to determine which method of constraining would result in the lowest axial loads. A 3.0-g deceleration in the vertical direction and a 1.0-g deceleration in each of two transverse directions was applied to the sphere and to the cylinder. The nodes restrained as shown in Figures 11 and 12 resulted in the lowest axial loads in the transition truss members for this transition truss configuration. The axial loads on the spherical tank and the cylinder struts range from -71,000 lb (-315.81 kN) to 160,000 lb (711.68 kN) and -34,000 lb (-151.23 kN) to 35,000 lb (155.68 kN), respectively.

# OF PAYLOAD CONSTRAINTS	PERCENTAGE OF LOADS IN SPECIFIED RANGE			
	$0 \leq X \leq 10,000$	$10,000 < X \leq 30,000$	$30,000 < X \leq 90,000$	$X > 90,000$
4	27.58%	40%	27.88%	4.55%
8	25.91%	31.97%	35%	7.12%
ALL	66.06%	33.94%	0	0

Figure 9. Variation of axial load.

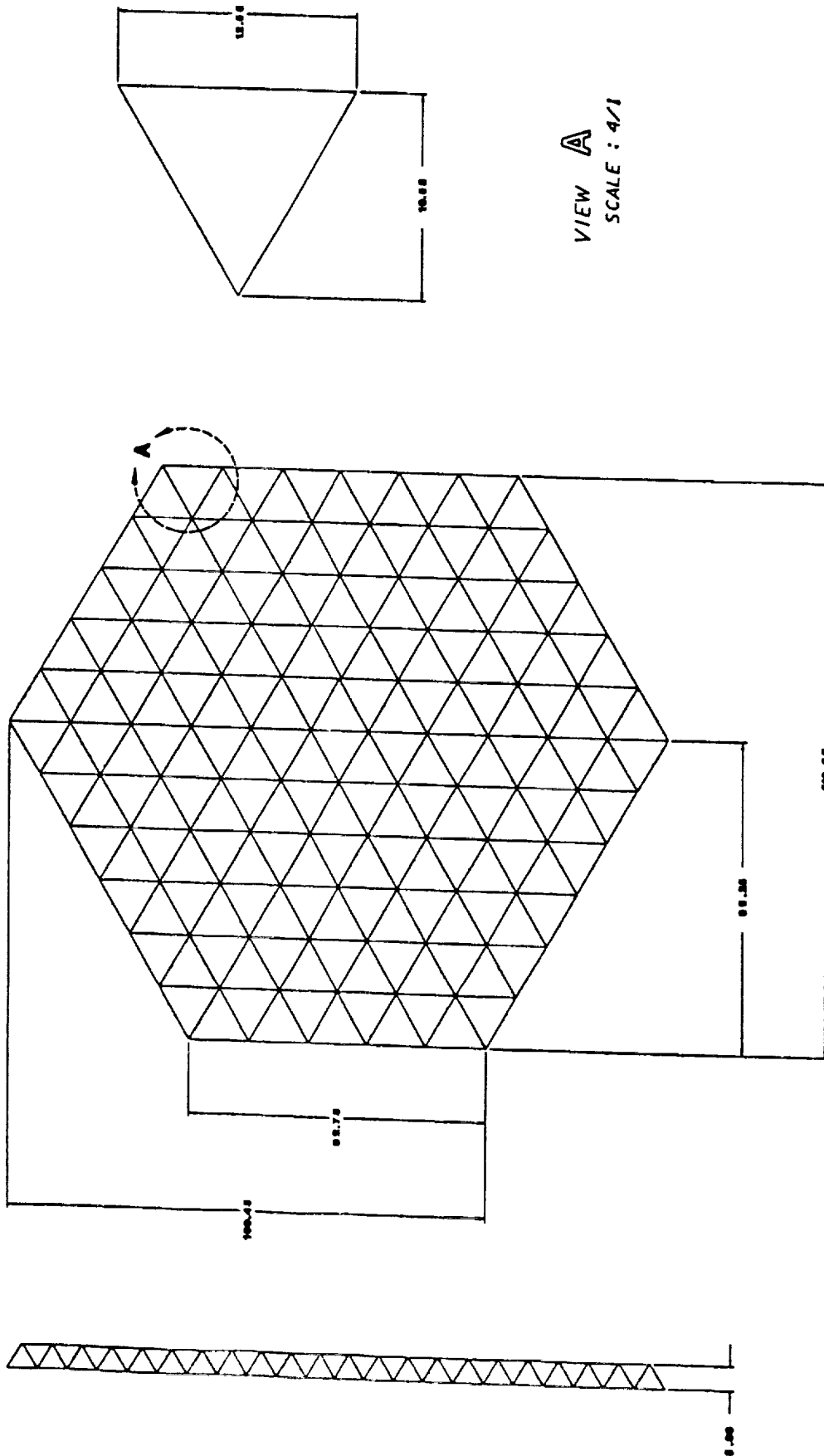


Figure 10. Transition truss – aerobrake support structure.

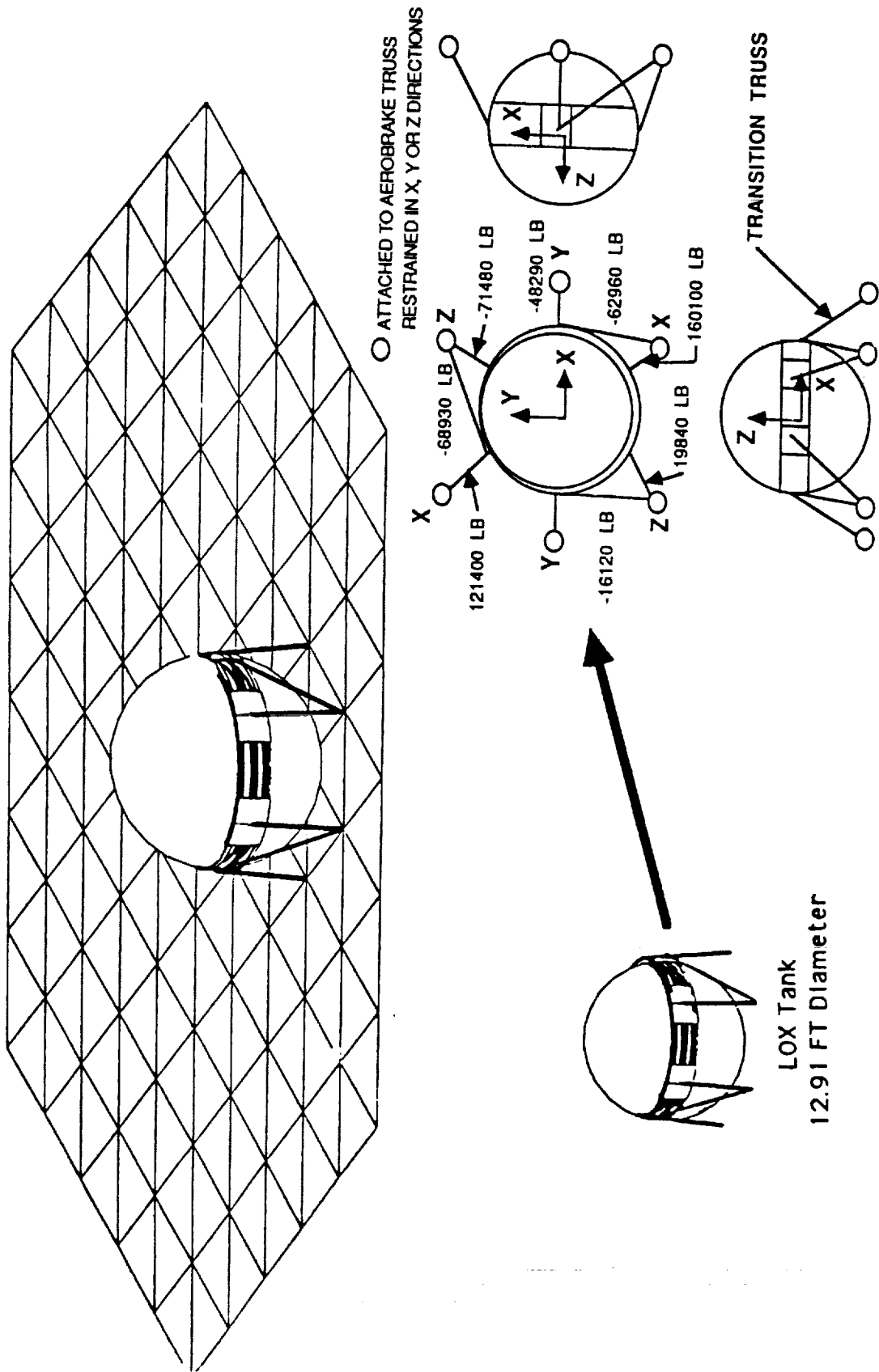


Figure 11. Transition truss – spherical components.

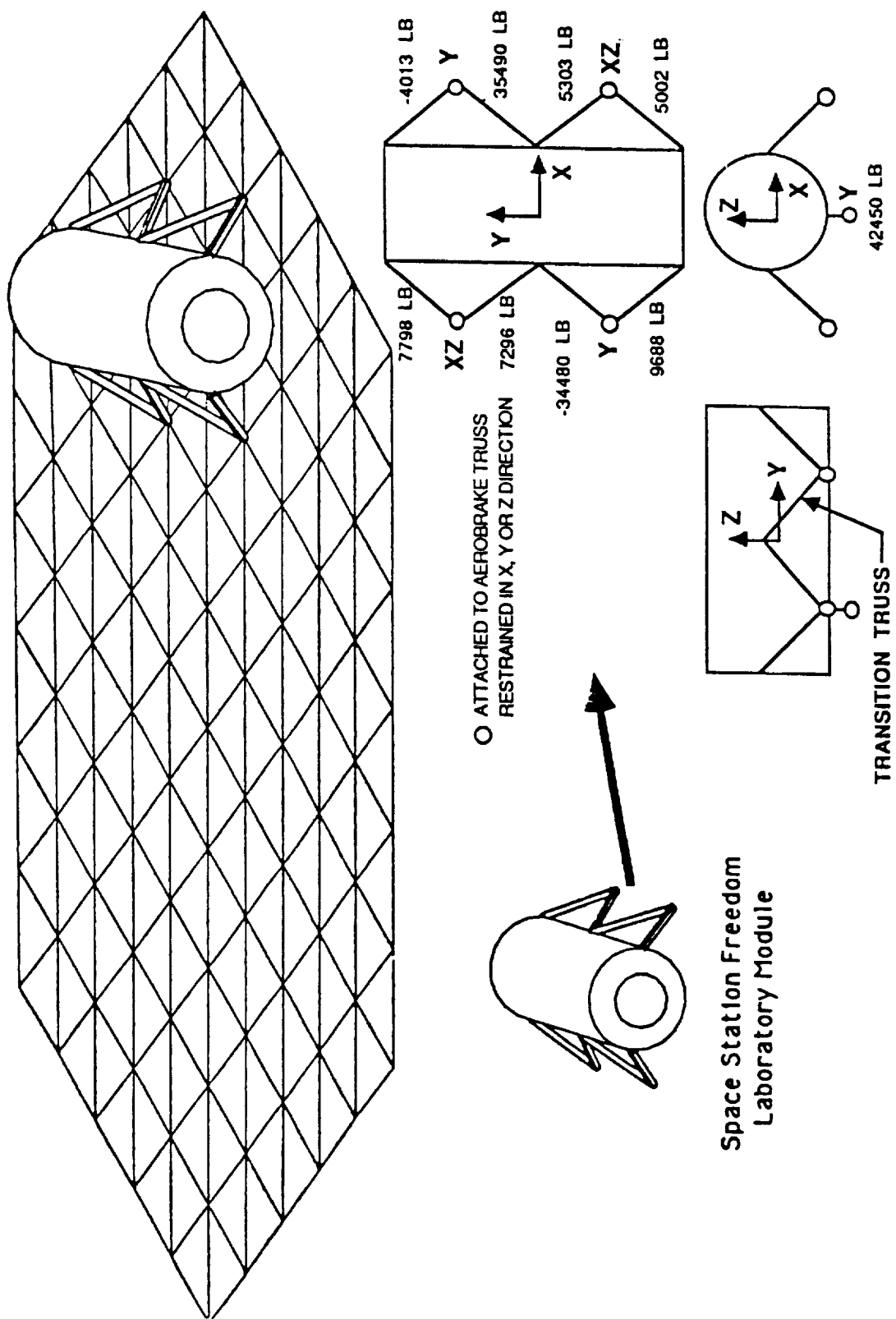


Figure 12. Transition truss - cylindrical components.

IV. LARGE COMPONENTS

The purpose of the large components task was to determine possible vehicle components for aerobrake attachment, including such components as fuel tanks, cryogenic tanks, pressurized habitation modules, liquid storage tanks, and unpressurized storage tanks. Once these types of components were identified, the size, shape, volume, mass, and thermal and radiation protection were determined as shown in Tables 1, 2, and 3. These components will be used in defining the axial loads in the transition truss that connects the components to the aerobrake (see Section III, Transition Truss). The specific details of the large components described were taken from previous interplanetary mission studies [2,3] that defined the size of tanks, modules, descent stages, etc., required for particular missions and aerobrake sizes. The propulsion system used on all the studies was LOX and liquid hydrogen (LH₂) with a mixture ratio of six to one. The tank weights include the total propellant used plus the additional amount needed to compensate for propellant boiloff during the assembly, checkout, and travel time to and from Mars.

The optimum pressure vessels for use in space vehicles are spherical but are limited in size by the existing transportation vehicles. In the aerobrake vehicle studies evaluated, the transportation vehicle varied with each study. To get a representative database, a single cargo vehicle (the Advanced Launch Vehicle) was baselined for use in this study which features a 43- and 45-ft (13.11-and 13.72-m) diameter cargo bay. Table 1 shows typical large components that might be required for a manned mission to Mars. These components would have to be assembled to the vehicle in low Earth orbit, checked out, transported to Mars, and then be used for the return trip to Earth. Table 2 shows typical large components that might be used to propel a manned vehicle toward Mars. These components would be attached to the vehicle, checked out on-orbit, then expended when the desired specific impulse was achieved. Tables 1 and 2 show the variation in sizes of LOX tanks and LH₂ tanks required to contain the "typical" volume of propellant required for planetary exploration missions, according to the referenced studies. These charts show the size difference between using a single LOX tank and LH₂ tank using a number of smaller diameter tanks that would carry the same propellant weight. Given these "typical" propellant volumes and tank sizes, the tank thickness and weight were then determined by assuming a low pressure pumped propellant storage tank. The design pressures for the LOX tank and LH₂ tank were 23 psi (158.58 kN/m²) and 50 psi (344.75 kN/m²), respectively.

Table 3 shows the typical insulation required for the propellant tanks for the journey to Mars. The tanks used to propel the vehicle out of low Earth orbit would require less insulation because the boiloff rate is comparatively small and the time these tanks are in use is comparatively short to those used in deep space.

V. MECHANICAL JOINTS

Much work has been devoted to the development of mechanical joint concepts for in-space construction and assembly. Initially, these concepts for attaching struts to truss nodal points were required to satisfy only two major criteria. First, the joint designs had to maintain sufficient

TABLE 1 LARGE COMPONENTS REQUIRED FOR EARTH DEPARTURE

REF	USE	ITEM	# TANKS	SHAPE	SIZE DIA (FT)	WEIGHT (LB)	VOLUME (FT ³)	TANK THK (IN)	TANK WT (LB)	TOTAL WT (LB)
MSFC	EARTH DEPARTURE	LOX	1	SPHERE	21.43	5149	367166	.041	879	6028
MSFC	EARTH DEPARTURE	LH2	1	SPHERE	30.18	14398	611946	.126	5333	19731
MSFC	EARTH DEPARTURE	LOX	6	SPHERE	11.79	858	61194	.023	146	1004
MSFC	EARTH DEPARTURE	LH2	6	SPHERE	16.61	2399	10199	.069	889	3288
MSFC	EARTH DEPARTURE	LOX	1	SPHERE	24.14	7366	525300	.046	1256	8622
MSFC	EARTH DEPARTURE	LH2	1	SPHERE	34.01	20598	87550	.142	7632	28230
MSFC	EARTH DEPARTURE	LOX	8	SPHERE	12.07	921	65662	.023	157	1078
MSFC	EARTH DEPARTURE	LH2	8	SPHERE	17.00	2572	10943	.071	953	3525
BOE	EARTH DEPARTURE	LOX	5	CYLIND	22.31X13.78	5387	244230	.043	991	6378
BOE	EARTH DEPARTURE	LH2	5	CYLIND	22.31X24.93	9748	37372	.093	2154	11902
BOE	EARTH DEPARTURE	LOX	5	SPHERE	18.17	3141	244230	.035	536	3676
BOE	EARTH DEPARTURE	LH2	5	SPHERE	25.60	8784	37372	.107	3255	12039
BOE	EARTH DEPARTURE	LOX	1	SPHERE	31.08	15725	1121148	.060	2680	18405
BOE	EARTH DEPARTURE	LH2	1	SPHERE	43.22	42275	186850	.180	15664	57938
MSFC	DEEP SPACE	LOX	1	SPHERE	12.89	1122	80138	.025	191	1313
MSFC	DEEP SPACE	LH2	1	SPHERE	18.17	3141	13356	.076	1164	4304
MSFC	DEEP SPACE	LOX	2	SPHERE	10.23	560	40069	.020	96	656
MSFC	DEEP SPACE	LH2	2	SPHERE	14.42	1569	6678	.061	582	2151
BOE	DEEP SPACE	LOX	1	CYLIND	18.84X19.68	5492	23341	.036	597	6089
BOE	DEEP SPACE	LH2	1	CYLIND	15.74X12.60	1964	140049	.066	757	2721
BOE	DEEP SPACE	LOX	1	SPHERE	15.54	1965	140049	.030	335	2300
BOE	DEEP SPACE	LH2	1	SPHERE	21.89	5492	23341	.091	2035	7527

MSFC-MARSHALL SPACE FLIGHT CENTER - MARS EXPLORATION SPLIT SPRINT MISSION
 BOE-BOEING - ANALYSES OF TECHNOLOGIES FOR MANNED LUNAR AND MARS MISSIONS



LARGEST LOX AND LH2 TANKS

TABLE 2. LARGE COMPONENTS REQUIRED FOR EARTH RETURN FROM MARS

REF	USE	ITEM	# TANKS	SHAPE	SIZE DIA (FT)	WEIGHT (LB)	VOLUME (FT^3)	TANK THK (IN)	TANK WT (LB)	TOTAL WT (LB)
MSFC	MARS DEPARTURE	LOX	1	SPHERE	12.91	80356	1126.62	.025	192.10	80548.10
MSFC	MARS DEPARTURE	LH2	1	SPHERE	18.18	13392	3146.16	.076	1165.78	14557.78
BOE	MARS DEPARTURE	LOX	1	SPHERE	15.15	129984	1820.70	.029	310.45	130294.45
BOE	MARS DEPARTURE	LH2	1	SPHERE	21.35	21664	5095.56	.089	1888.12	23552.12
BOE	MARS DEPARTURE	LH2	2	SPHERE	11.75	10832	2548.68	.049	314.74	11146.74
MSFC	MARS DEPARTURE	LOX	2	SPHERE	10.25	40176	563.86	.020	96.14	40272.14
MSFC	MARS DEPARTURE	LH2	2	SPHERE	14.44	6696	1576.52	.060	584.17	7280.17
OTV	MARS DEPARTURE	LOX	1	SPHERE	10.75	46436	651.27	.021	110.91	46546.9
OTV	MARS DEPARTURE	LH2	1	SPHERE	14.95	7739	1750.0	.062	648.28	8387.28
OTV	MARS DEPARTURE	LOX	2	SPHERE	8.53	23218	325.63	.016	55.41	23273.41
OTV	MARS DEPARTURE	LH2	2	SPHERE	11.86	3870	875.0	.050	323.66	4193.66
AMES	LANDER	LDR	1	AERO	N/A	65599	N/A	N/A	N/A	65599
DAURO	LANDER	LDR	1	AERO	N/A	135000	N/A	N/A	N/A	13500
MSFC	LANDER	LDR	1	AERO	54	133047	N/A	N/A	N/A	133047
BOE	LANDER	LDR	1	AERO	85X65	65898	N/A	N/A	N/A	65898
SSF	HABITATION	MOD	1	CYLIN	42X14.5	44463	1913.23	N/A	N/A	44463
SSF	LABORATORY	MOD	1	CYLIN	42X14.5	60920	1913.23	N/A	N/A	60920
SSF	LOGISTICS (PRESSURIZED)	MOD	1	CYLIN	21.8X14.5	16853	993.06	N/A	N/A	16853
SSF	NODE	NODE	1	CYLIN	15.5X14.5	14954	719.74	N/A	N/A	14954
SSF	LOGISTICS (UNPRESSURIZED)	MOD	1	DISK	14.5X8	3034	364.42	N/A	N/A	3034

MSFC-MARSHALL SPACE FLIGHT CENTER - MARS EXPLORATION SPLIT SPRINT MISSION

BOE-BOEING - ANALYSES OF TECHNOLOGIES FOR MANNED LUNAR AND MARS MISSIONS

OTV- MARTIN MARIETTA - ORBITAL TRANSFER VEHICLE CONCEPT DEFINITION AND SYSTEM ANALYSIS STUDY

DAURO- V. A. DAURO - AEROBRAKING; SSF- SPACE STATION FREEDOM (BOEING)

AMES- AMES RESEARCH CENTER - HIGH ENERGY AEROBRAKE (HEAB) WORKSHOP



LARGEST LOX AND LH2 TANKS

TABLE 3. LARGE COMPONENTS THERMAL AND RADIATION PROTECTION

PROGRAM	MISSION	INSULATION (INCHES)		DAYS IN ORBIT	BOILOFF RATE (LB/HR)/%
		LOX	LH2		
SPLIT SPRINT	GROUND ASSEMBLED	1/2 MLI	1/2 MLI, 1/2 SOFI*	847	.430 / 9.41
SPLIT SPRINT	SPACE ASSEMBLED	1/2 MLI	1/2 MLI, 1/2 SOFI	908	.445 / 10.34
AOTV	GROUND ASSEMBLED	1/2 MLI	1/2 MLI, 1/4 SOFI	20	2.8** / 4.52***
AOTV	SPACED ASSEMBLED	1 MLI	1 MLI	20	2.8 / 4.52
BOEING	MARS RETURN	2 MLI	4 MLI	363.3	.325 / 8.01
BOEING	VENUS SWINGBY	2 MLI	4 MLI	130.3	.246 / 2.29

*SOFI-SPRAY-ON FOAM INSULATION

**ASSUMED BOILOFF RATE

*** LUNAR MISSION, GEO=17200 NMI, 5000 LB PAYLOAD UP, 0.0 LB PAYLOAD DOWN

RADIATION PROTECTION SHALL BE 10.25 LB/FT^2 (5gm/cm^2) FOR THE CREW
(OFFICE OF EXPLORATION STUDY REQUIREMENTS DOCUMENT FY 1989 STUDIES
SECTION 2.4.4.2.2.4.4)

strength in order to withstand aerobrake induced loads of 100,000 lb (444.80 kN) in tension or compression. Second, they had to have the capability of being assembled from the side. These preliminary conditions are still valid; however, more mechanical joint requirements have evolved and have been incorporated accordingly into the following joint designs. All joints are composed of two parts: the connector and receptacle. The connector is attached to the strut and the receptacle is attached to the node.

A. Threaded Truss Joint

The first mechanical joint, the threaded truss joint, that was designed is displayed in Figure 13. In this particular design, an outer alignment joint surrounds a stronger mechanically driven threaded joint. This joint was designed to meet the 100,000-lb (444.80-kN) axial load and robot assembly requirements. The assembly of this joint requires the robot to perform two operations—place the element near the attachment location and turn a bolt. A temporary outer alignment feature holds the position of the element after it has been placed near the receptacle, then a robot turns a standard hex head bolt. However, after this joint design was in its final stages, a new requirement was established. The mechanical joint needs the capability to adjust node centers from a ± 0.020 -in (± 0.0508 -cm) axial misalignment within a truss structure to a “true” position. This joint was modified (Fig. 14) to meet this requirement by redesigning the temporary alignment sleeve, and providing tapered surfaces to push the element into position. As the threaded section is rotated, the tapered surfaces on the threaded section force the element end up or down against the tapered surfaces on the tube end. The tapered surfaces on the tube transfer the force into an axial load, pushing the element into the correct position. These modifications required an excessive number of parts, and made the assembly torque prohibitively high, approximately 4,000 in-lb (45,192 N-m) Also, these redesigns made the joint longer and consequently heavier. For these reasons the threaded truss joint was deemed too complicated and was shelved.

B. Grip Joint

The second concept, the grip joint, was designed to the requirements of robotic assembly, $\pm 100,000$ -lb (444.80-kN) axial load and a ± 0.020 -in (± 0.0508 -cm) misalignment correction and is shown in Figure 15 and 16. The assembly of the joint requires a robot to perform the same two operations as for the threaded truss joint—placing the element and turning a bolt. As the robot brings the element near its final position, the bolt engages a “zip nut[®],” and the joint’s grooves become roughly lined up. Then the robot turns a standard hex head bolt aligning the connector and receptacle to the final “true” position.

The “zip nut[®]” is an independently designed and patented nut, in which the threads are cut into three segments and spring loaded. This allows a bolt to be pushed into it, then tightened by a single rotation. This not only reduces assembly time by saving the robot 30 or 40 revolutions of an end effector, but saves weight by eliminating a temporary alignment feature such as that in the threaded truss joint.

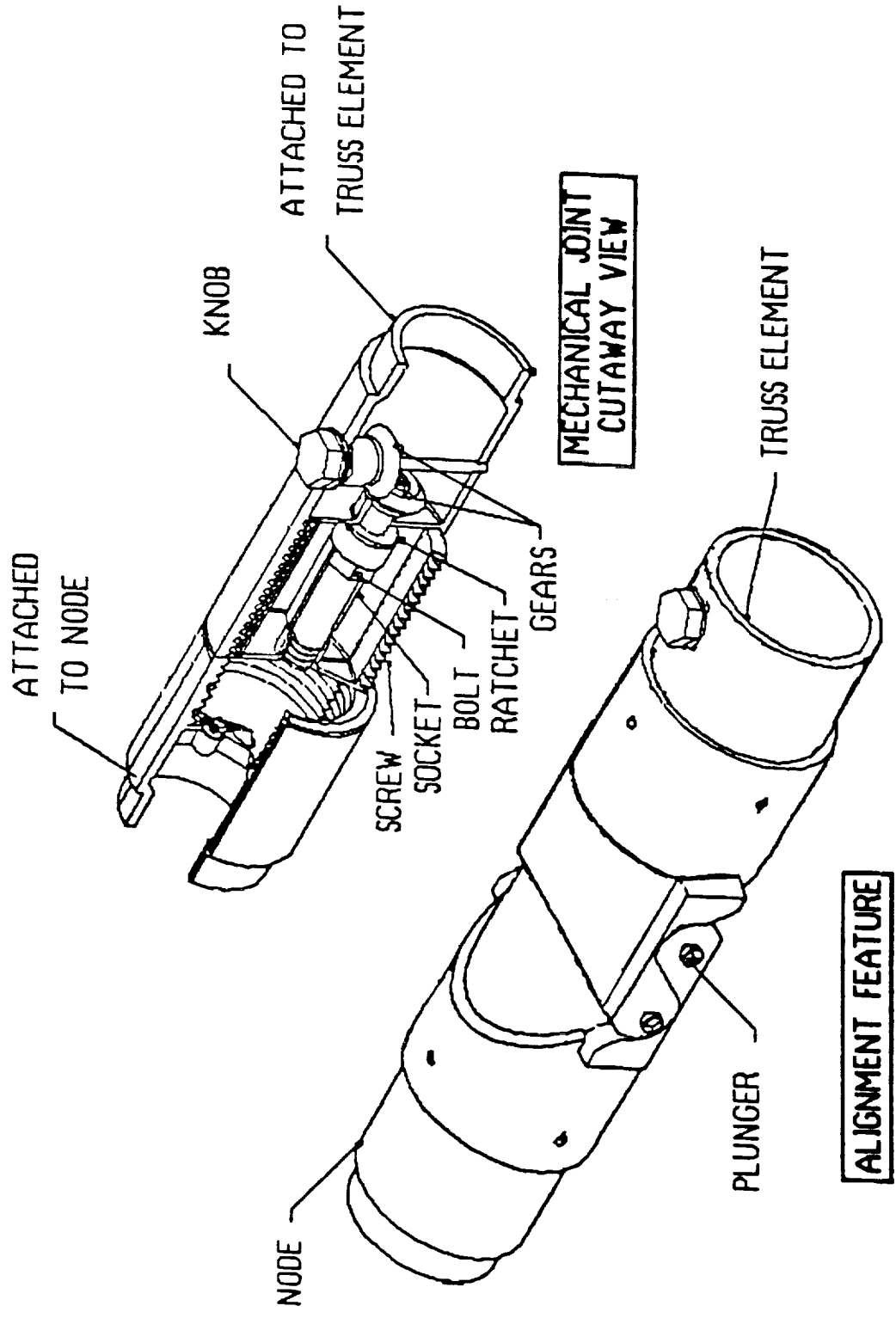
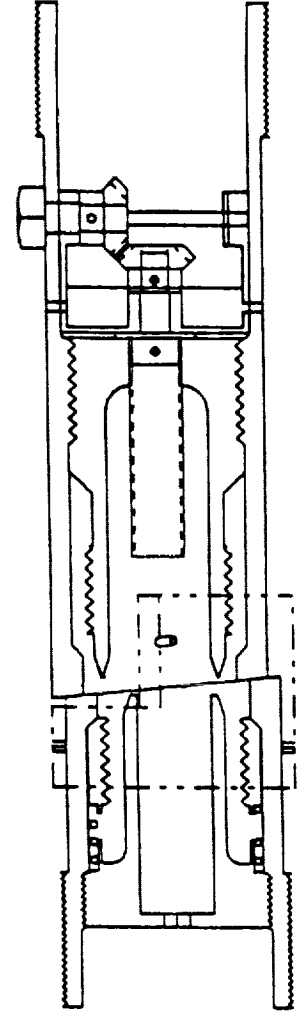
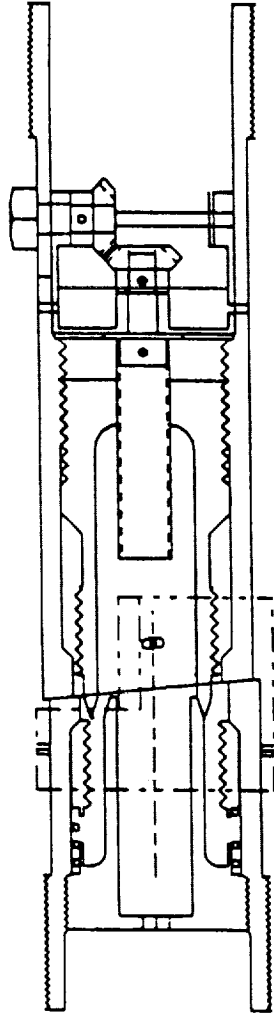


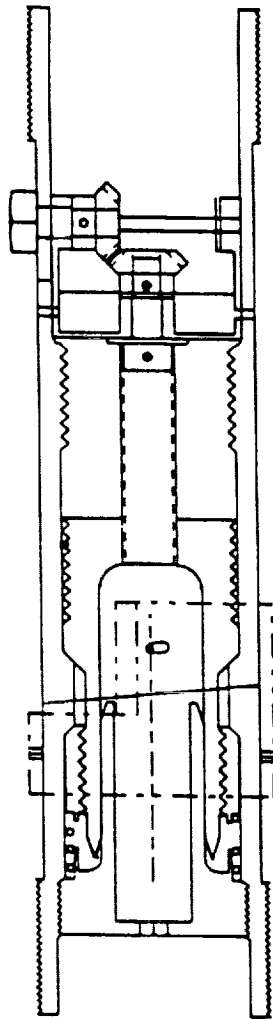
Figure 13. Threaded screw joint.



INITIAL POSITION



JOINT ASSEMBLY



MATED POSITION

Figure 14. Threaded screw joint mating sequence.

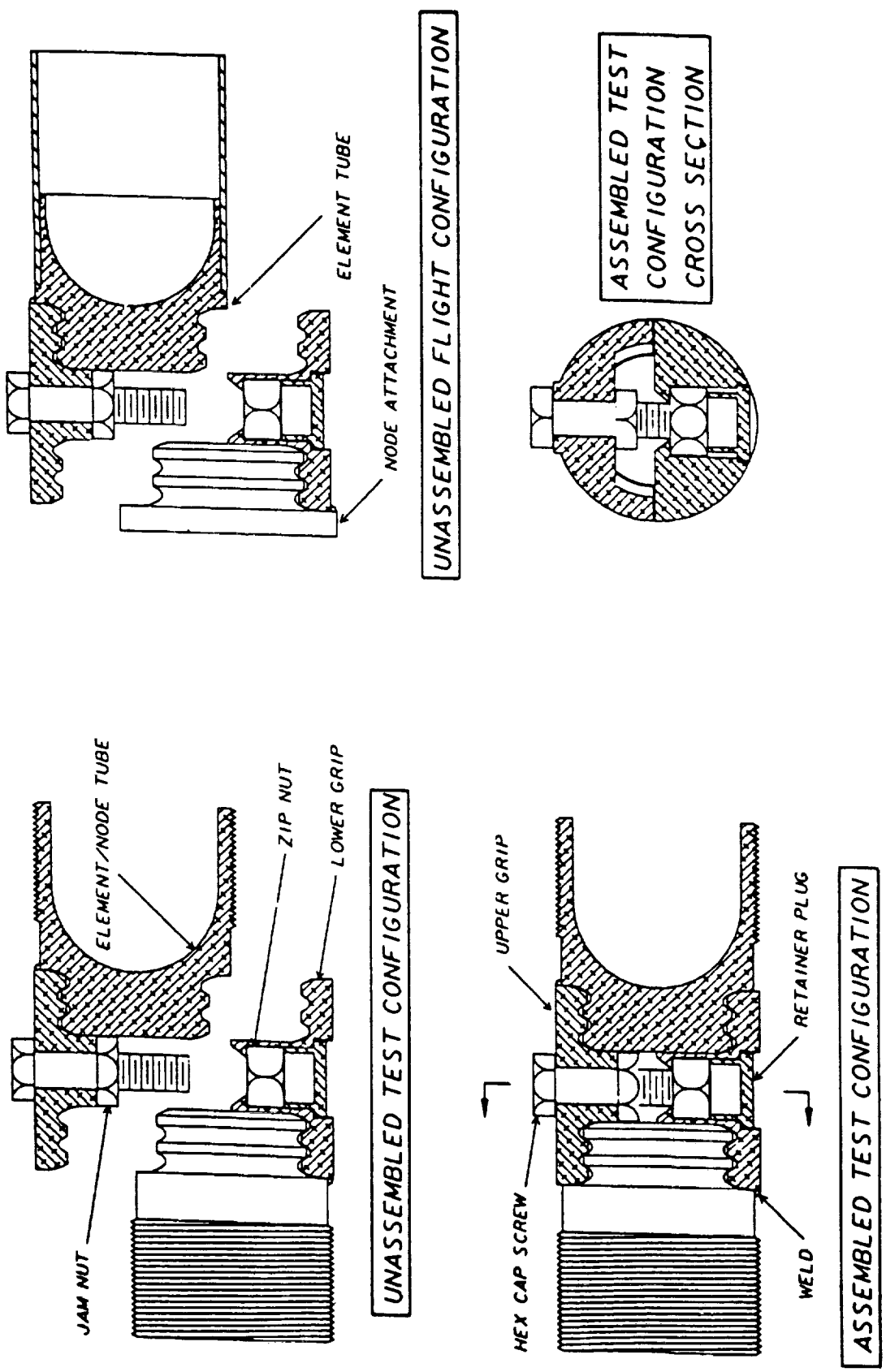


Figure 15. Grip joint configuration.

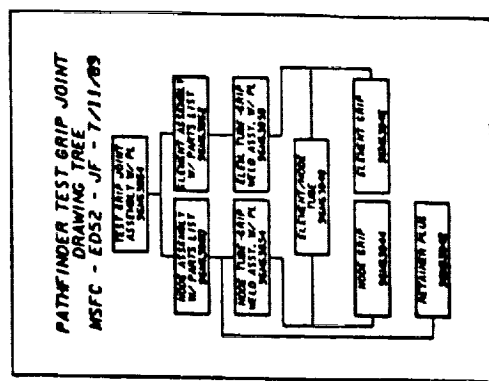
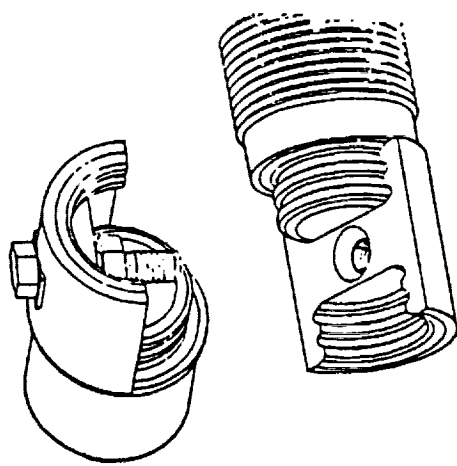
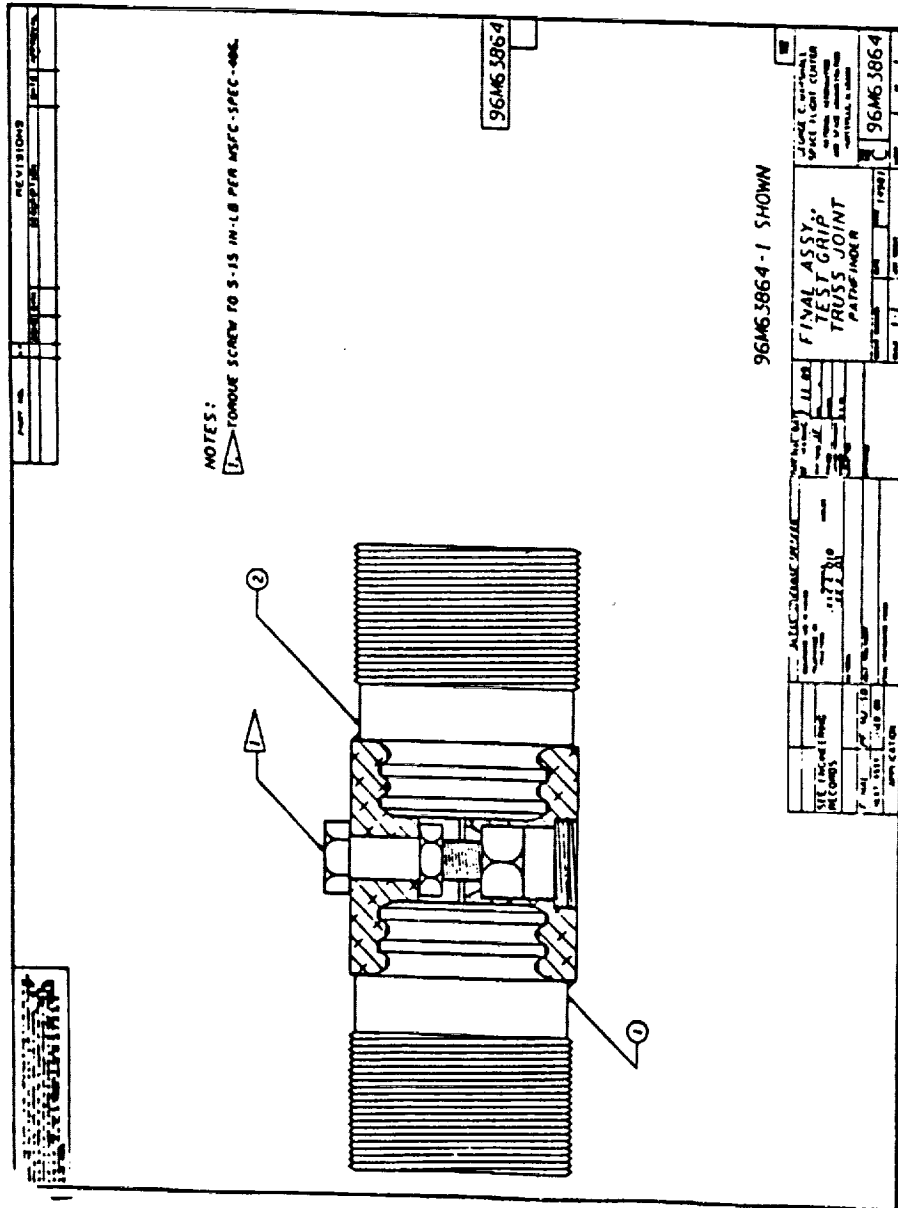


Figure 16. Grip joint.

As the bolt is tightened, its tension pulls the axisymmetric inclined planes of the grooves together. The inclined planes transfer the vertical force to the bolt into an axial force which stretches or compresses the element until it is in the correct position. The maximum axial load required to position the elements is about 5,000 lb (22.24 kN), found by the elastic deformation of a beam under axial loading.

There were several design considerations in this joint: shear area of the grooves, stress concentrations caused by the grooves, bolt loading and torque requirements, bending moments along the axis of the gripper sections, and bending moments acting to open the semicircular gripper sections (large moments could be countered by adding tabs on the edges of the element and node that would prevent gripper section deformation past a certain point).

The grip joint, while not having been optimized, is now being built out of several materials including 2219-T87 aluminum, titanium 6A14V alloy, and an "isotropic" 20-percent silicon carbide aluminum 2124 metal matrix composite. The grip joint is being fabricated from these materials to determine which material will optimally meet the strength, weight, and coefficient of thermal expansion requirements established for in-space assembly and construction. Tension and torque tests are scheduled to be performed in early CY 1990. Tension and compression tests in a thermal vacuum chamber may be scheduled if preliminary test results are positive.

C. Clevis Joint

The third mechanical joint, the clevis joint, is displayed in Figure 17. This design incorporates a tang and clevis concept. As the bolt engages the "zip nut[®]," the two cones are pulled into a locked position, thus producing a double wedge effect. Further analysis of this joint yielded mechanical and fabrication complexities which resulted in shelving the concept.

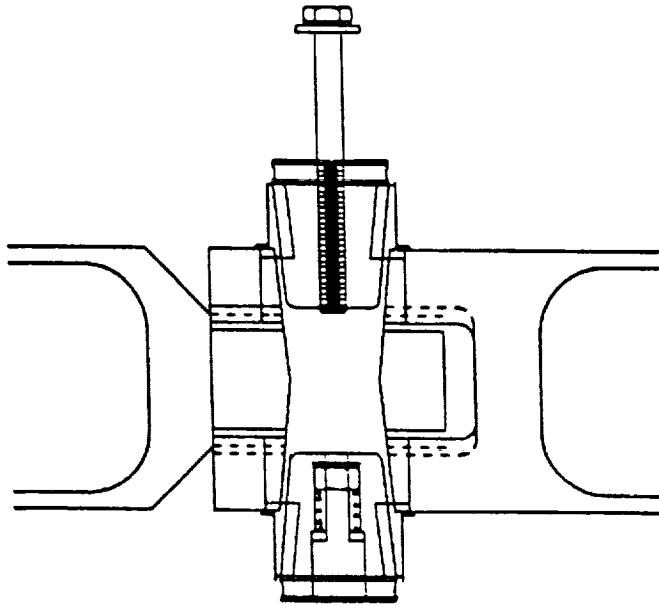
D. Slip Joint

The fourth concept, the slip joint, is pictured in Figure 18. This design is still undergoing preliminary analysis and feasibility studies. Both halves of the joint are conically shaped and are wedged into a locked position by the bolt engaging a "zip nut[®]." Two new mechanical joint requirements are being applied to this current concept. First, the joint must be disassembled as easily as it is assembled. Second, not only should the joint possess the capability of being assembled by a robot, but by an astronaut as well. Much more work is required to solidify this concept.

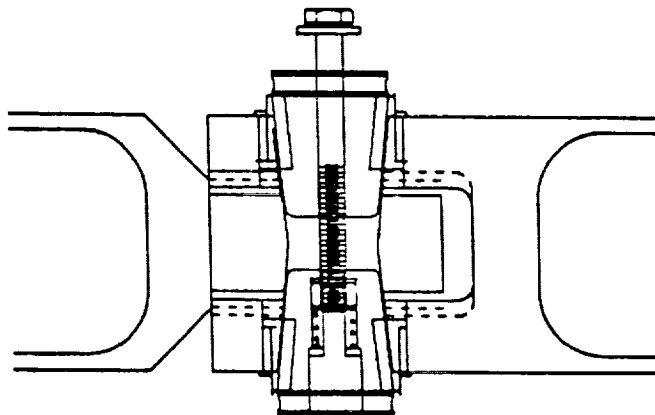
VI. CONCLUSION

A generic space structure for studying in-space assembly and construction was developed by NASA to determine the technology required for building large structures in space. The space structure defined was a 120-ft (36.57-m) diameter aerobrake, i.e., thermal insulation supported by a tetrahedral truss with manned facilities and engines attached to the tetrahedral truss. An analysis of

INITIAL
PLACEMENT



TEMPORARY
ALIGNMENT



MATED
POSITION

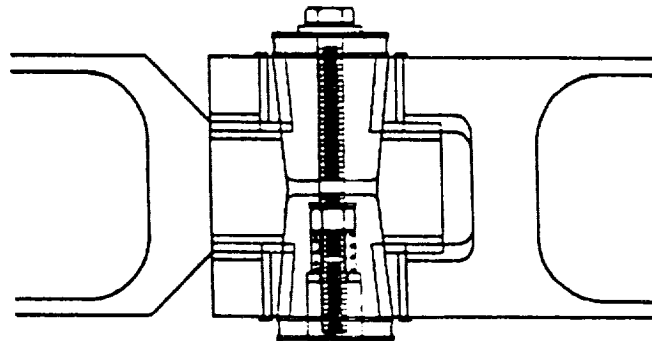


Figure 17. Clevis joint mating sequence.

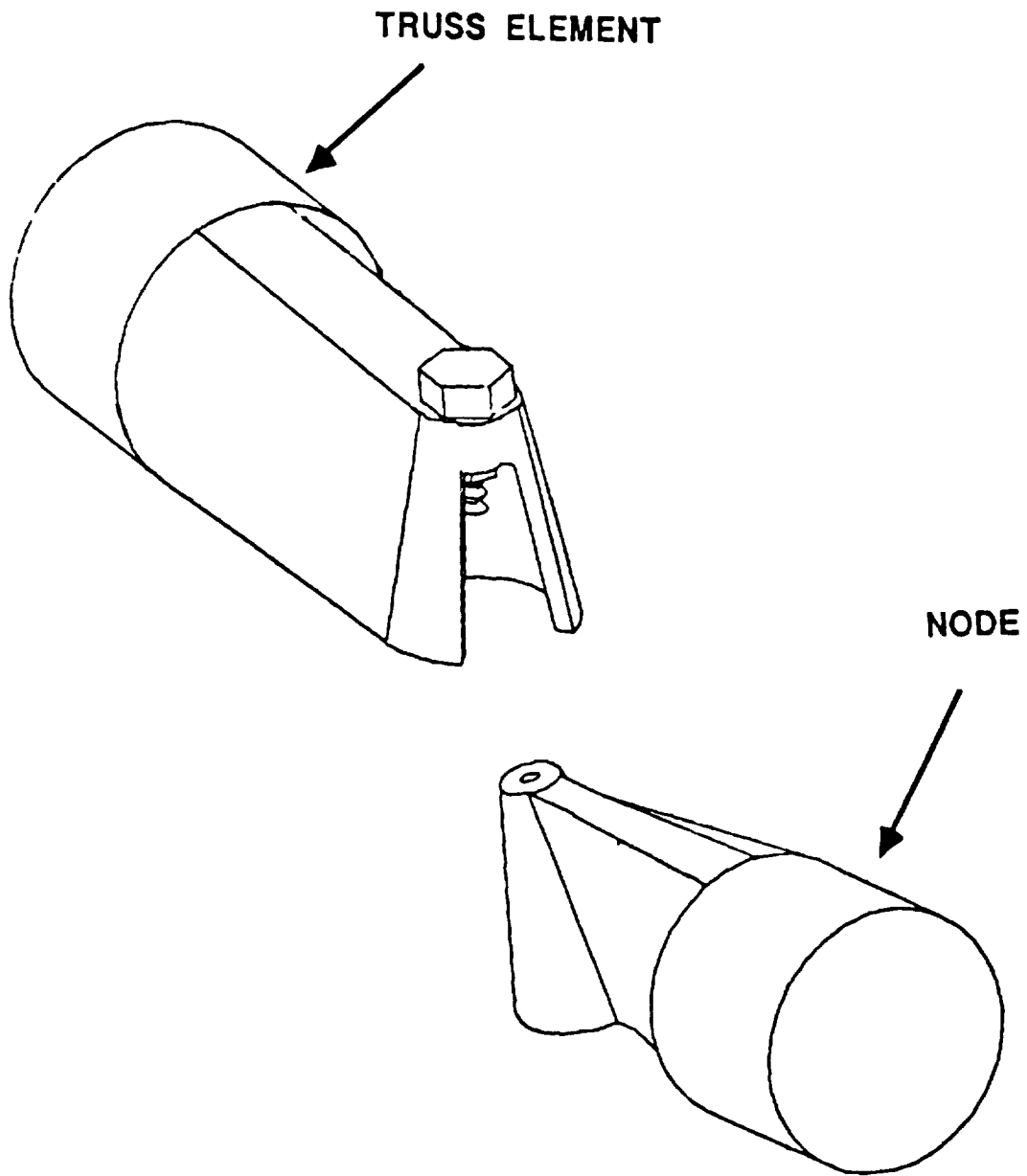


Figure 18. Slip joint.

the structure was performed to define load requirements for the design of mechanical joining methods. Four methods of mechanically connecting truss elements via a robot were investigated. One, the grip joint, was designed and is being built.

Research was initiated to define the types of large components that might be attached to the aerobrake for interplanetary missions. A task was performed to determine an optimum method of attaching the components to the tetrahedral truss. Two large components, a 12.91-ft (3.94-m) diameter LOX tank and a 42 by 14.5-ft (12.8 by 4.42-m) Space Station Freedom laboratory module, were used to define loads and attachment schemes for connecting these components to the tetrahedral truss.

REFERENCES

1. Boeing, Marshall Space Flight Center, "Analysis of Technologies for Manned Lunar and Mars Missions." Contract NAS8-137. NASA-Marshall Space Flight Center, 1989.
2. NASA-Marshall Space Flight Center, "Mars Exploration—Split Sprint Mission Low Earth Orbit Assembly Versus Ground Assembly." NASA-Marshall Space Flight Center, April 1989.
3. Martin Marietta, NASA-Marshall Space Flight Center, "Orbital Transfer Vehicle Concept Definition and System Analysis Study." NASA-Marshall Space Flight Center, October 1985.
4. FED-STD-H28/2A, April 1984. Table II.B.1 Formulas for Screw Thread Strength Factors.

BIBLIOGRAPHY

Boeing, NASA-Ames, "Engineering Analysis for Assembly and Checkout of Space Transportation Vehicles in Orbit." NASA-Ames Research Center, October 20, 1989.

Dauro, V.A.: "Aerobraking." NASA Report No. N87-17784. Marshall Space Flight Center, 1987.

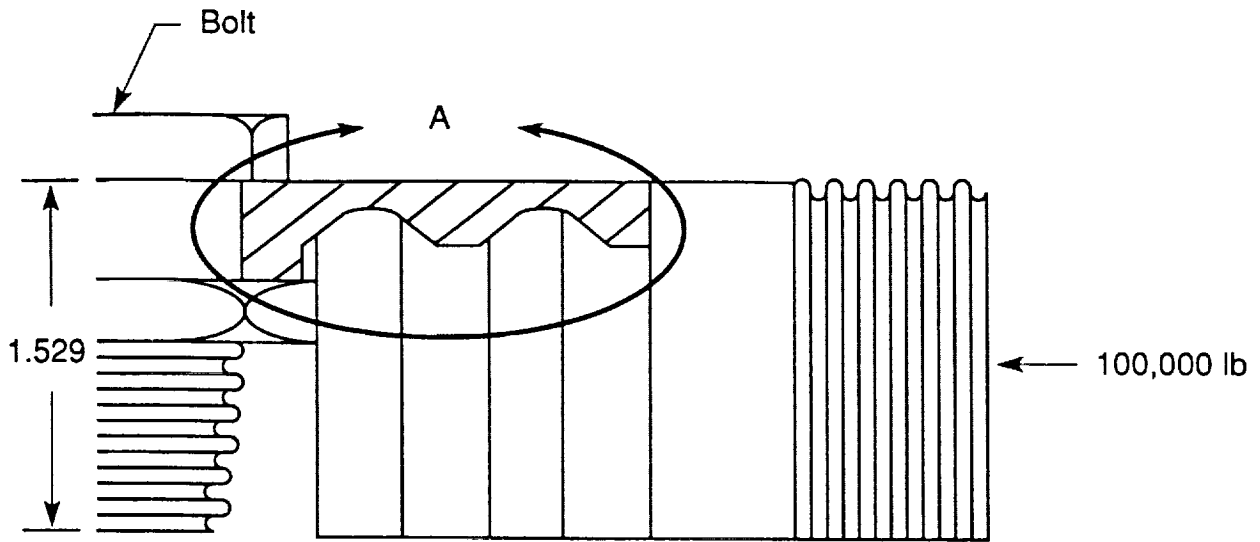
Hill, O., and Wallace, R.: "Manned Mars Mission Vehicle Design Requirements for Aerocapture." NASA-Johnson Space Center, Report No. N87-17781.

Hoffmen, S.J.: "A Comparison of Aerobraking and Aerocapture Vehicles for Interplanetary Missions." NASA Headquarters contract No. NASW-3622.

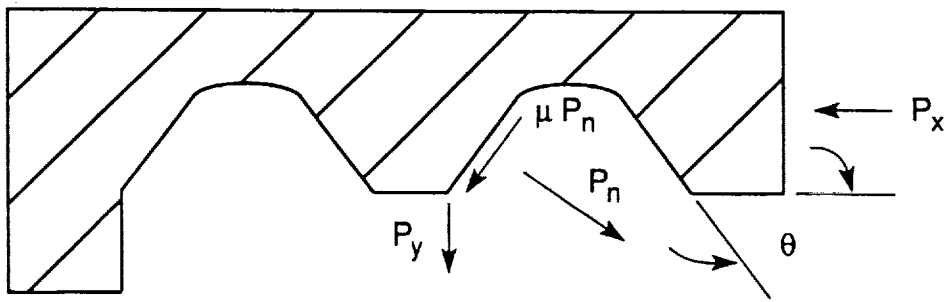
Meenes, G.P.: "Aeroassisted-Vehicle Design Studies for a Manned Mars Mission." 38th Congress of the IAF, Report No. IAF/IAA-87-433, NASA Report No. A88-16097.

Park, C.: "A Survey of Aerobraking Orbital Transfer Vehicle Concepts." AIAA 25th Aerospace Sciences Meeting, Report No. AIAA-87-0514, NASA Report No. A87-22619.

APPENDIX A



Flat Plate Analogy



View A

$P_x=100,000$ lb
 P_y =BOLT LOAD
 $\theta=60^\circ$

R=1.529 inches

3/4" bolt, F_{tu} = MINIMUM TENSILE STRENGTH 126,758 psi per MS90727

Assumption: $\mu = .10$

$$\Sigma F_x = 0 \quad P_x - P_n \text{SIN } \theta - \mu P_n \text{COS } \theta = 0$$

$$P_n = \frac{P_x}{\text{SIN } \theta + \mu \text{COS } \theta}$$

$$P_n = \frac{100,000}{\text{SIN } 60^\circ + .1(\text{COS } 60^\circ)} = 109,167 \text{ lbs}$$

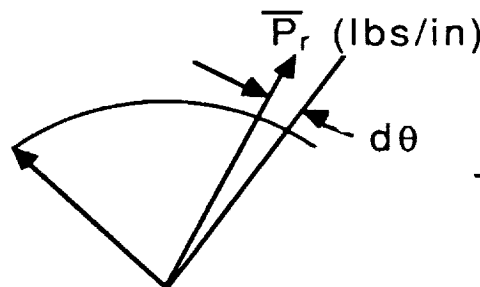
$$\Sigma F_y = 0 \quad P_y + \mu P_n \text{SIN } \theta - P_n \text{COS } \theta = 0$$

$$P_y = P_n (\text{COS } \theta - \mu \text{SIN } \theta)$$

$$P_y = 109,167 (\text{COS } (60^\circ) - (.1) \text{SIN } (60^\circ))$$

$$P_y = 45,129 \text{ lbs}$$

Calculation of the bolt load, P_y , assumed a flat plate. However, the part is actually a circle.



$$P_y = \bar{P}_r (2 \pi R)$$

$$\bar{P}_r = \frac{45,129}{2\pi (1.529)}$$

$$\bar{P}_r = 4,698 \text{ lb/in}$$

P_y^* is defined as the actual bolt load on the circular section of the joint.

$$P_y^* = \bar{P}_r \cos \theta ds = \bar{P}_r \cos \theta R d\theta$$

$$P_y^* = 4\bar{P}_r R \int_0^{90} \cos \theta d\theta = 2\bar{P}_r R$$

$$P_y^* = 4(4,698 \text{ lbs/in})(1.529 \text{ in}) = 28,733 \text{ lbs}$$

Margin of Safety (Bolt):

$$\sigma_{tu \text{ bolt}} = 56,000 / [\pi (.375^2)] = 126,758 \text{ psi}$$

$$\sigma^* = P_y^* / \text{Area of } 3/4" \text{ bolt} = 28,733 / [\pi (.375^2)] = 65,038 \text{ psi}$$

$$\text{M.S.} = \frac{\sigma_{tu \text{ bolt}}}{\text{F.S. } \sigma^*} - 1 = \frac{126,758}{1.4(65,038)} - 1 = +0.39$$

SHEAR AREA OF EXTERNAL THREADS (NUT):

$$\text{Area} = \Pi n L_e K_{n(\max)} \left[\frac{1}{2n} + 0.57735 (E_{s(\min)} - K_{n(\max)}) \right]^{(4)}$$

where: n = Number of threads per inch = 16

L_c = Length of thread engagement $\cong 3/4$ in (scaled)

$K_{n(\max)}$ = Maximum minor diameter of internal threads = 0.6908 in

$E_{s(\min)}$ = Minimum pitch diameter of external threads = 0.7079 in

$$F_{su} = 0.57 (F_{tu}) = 0.57 (126,758) = 72,252 \text{ psi}$$

$$\begin{aligned} \text{Area} &= \Pi (16) (3/4) (0.6908) \left[\frac{1}{2(16)} + (0.57735) \right. \\ &\quad \left. (0.7079 - 0.6908) \right] \\ &= 1.07 \text{ in}^2 \end{aligned}$$

$$\sigma = P y^* / \text{Area} = 28,733 \text{ lbs} / 1.07 \text{ in}^2 = 26,850 \text{ psi}$$

$$\text{M.S.} = 72,252 / [(1.4) (26,850)] - 1 = +0.92$$

SHEAR AREA OF INTERNAL THREADS (BOLT):

$$\text{Area} = \Pi n L_e D_{s(\min)} \left[\frac{1}{2n} + 0.57735 (D_{s(\min)} - E_{n(\max)}) \right]$$

where: $D_{s(\min)}$ = minimum major diameter of external threads = 0.7406 in

$E_{n(\max)}$ = maximum pitch diameter of internal threads = 0.7179 in

$$\text{Area} = \Pi(16) (3/4) (0.7406) [1/ (2(16) + 0.57735 (0.7406 - 0.7179))] = 1.238 \text{ in}^2$$

$$\sigma = P y^* / \text{Area} = 28,733 \text{ lbs} / 1.238 \text{ in}^2 = 23,209 \text{ psi}$$

$$\text{M.S.} = [72,252 / (1.4) (23,209)] - 1 = +1.22$$

SHEAR AREA OF INTERNAL THREADS (NODE TUBE):

$$\text{Area} = \Pi n L_e D_{s(\text{min})} [1/(2n) + .57735 (D_{s(\text{min})} - E_{n(\text{max})})]$$

$$n = 2$$

$$L_e = 1.341 \text{ in}$$

$$D_{s(\text{min})} = 3.115 \text{ in}$$

$$E_{n(\text{max})} = 2.9325 \text{ in}$$

$$F_{su} = 34,000 \text{ psi per MIL- HDBK-5E, table 3.2.6.0 (c)}$$

$$\text{Area} = \Pi(2) (1.341) (3.115) [1/ (2(2) + 0.57735 (3.115 - 2.9325))] = 9.327 \text{ in}^2$$

$$\sigma = F / \text{Area} = 100,000 \text{ lbs} / 9.327 \text{ in}^2 = 10,722 \text{ psi}$$

$$\text{M.S.} = [34,000 / (1.4) (10,722)] - 1 = +1.26$$

SHEAR AREA OF EXTERNAL THREADS (NODE TUBE):

$$\text{Area} = \Pi n L_e K_{n(\text{max})} [1/(2n) + 0.57735 (E_{s(\text{min})} - K_{n(\text{max})})]$$

$$n = 2$$

$$L_e = 1.341 \text{ in}$$

$$K_{n(\max)} = 2.745 \text{ in}$$

$$E_{s(\min)} = 2.93 \text{ in}$$

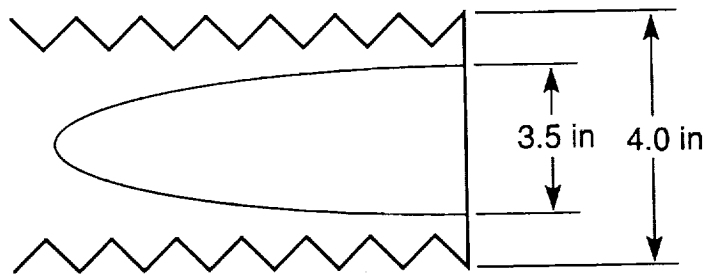
$$F_{su} = 34,000 \text{ psi per MIL- HDBK-5E, table 3.2.6.0 (c)}$$

$$\text{Area} = \Pi(2) (1.341)(2.745) [1/ (2(2) + 0.57735 (2.93 - 2.745))] \\ = 8.2525 \text{ in}^2$$

$$\sigma = F / \text{Area} = 100,000 \text{ lbs} / 8.2525 \text{ in}^2 = 12,118 \text{ psi}$$

$$\text{M.S.} = [34,000 / (1.4) (12,118)] - 1 = +1.00$$

THIN TUBE SECTION (NODE TUBE)



$$\text{Area} = \Pi/4 [(4.0)^2 - (3.5)^2] = 2.9452 \text{ in}^2$$

$$\sigma = 100,000 \text{ lbs} / 2.9452 \text{ in}^2 = 33,954 \text{ psi}$$

$$\text{F.S.} = 1.1 \text{ on yield}$$

$$F_{cy} = 40,000 \text{ psi per MIL-HDBK- 5E, table 3.2.6.0 (c)} \\ \text{(for T852)}$$

$$M.S. = [40,000 / (1.1) (33,954)] - 1 = +.07$$

SHEAR AREA OF EXTERNAL THREADS

$$\text{Area} = \Pi n L_e K_n(\text{max}) [1/(2n) + 0.57735 (E_s(\text{min}) - K_n(\text{max}))]$$

$$n = 8$$

$$L_e = 1/2 (2.5) = 1.25 \text{ in (assumed 1/2 of length of threads)}$$

$$K_n(\text{max}) = 4.0 \text{ in}$$

$$E_s(\text{min}) = 4.125 \text{ in}$$

$$F_{su} = 34,000 \text{ psi per MIL- HDBK-5E table 3.2.6.0 (c)}$$

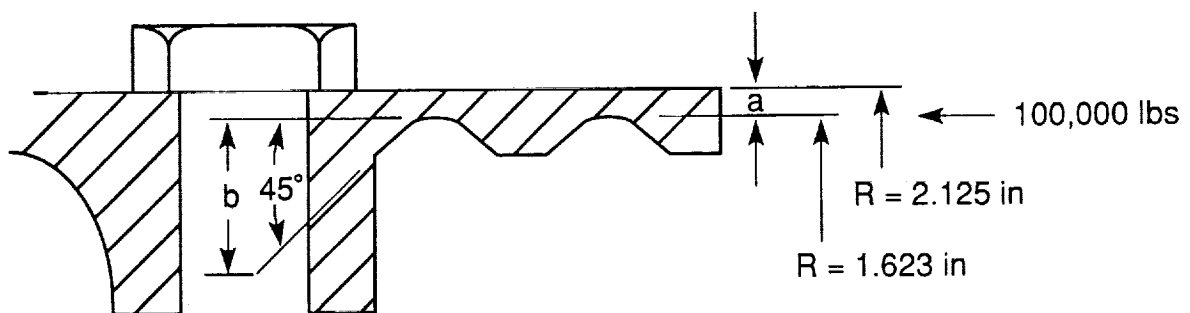
$$\text{Area} = \Pi (8) (1.25) (4.0) [1/(2)(8) + 0.57735 (4.125 - 4.0)]$$

$$= 16.923 \text{ in}^2$$

$$\sigma = F / \text{Area} = 100,000 \text{ lbs} / 16.923 \text{ in}^2 = 5,909 \text{ psi}$$

$$M.S. = [34,000 / (1.4) (5,909)] - 1 = +3.11$$

STRESS AROUND BOLT HOLE:



b = 9/16 in (.5625) scaled from drawing

$$\text{Area} = \text{Area}_a + \text{Area}_b$$

$$\begin{aligned} \text{Area} &= \Pi \{ [(2.125)^2 - (1.623)^2] + [(1.623)^2 - (1.623 - .5625)^2] \} \\ &= 10.65 \text{ in}^2 \end{aligned}$$

$$\sigma = F / A = 100,000 / 10.65 = 9,389 \text{ psi}$$

Assuming a stress concentration factor of 3.0 around the hole,

$$\sigma_{\text{hole}} = 3.0 (9,389) = 28,170 \text{ psi}$$

$$\text{for } F_{\text{tu}} = 56,000 \text{ psi}$$

$$\text{M.S.} = [56,000 / (1.4) (28,170)]^{-1} = +.42$$

$$\text{for } F_{\text{cy}} = 40,000 \text{ psi}$$

$$\text{M.S.} = [40,000 / (1.1) (28,170)]^{-1} = +.29$$

APPROVAL

DEFINITION OF LARGE COMPONENTS ASSEMBLED ON-ORBIT AND ROBOT COMPATIBLE MECHANICAL JOINTS

By J. Williamsen, F. Thomas, J. Finckenor, and B. Spiegel

The information in this report has been reviewed for technical content. Review of any information concerning Department of Defense or nuclear energy activities or programs has been made by the MSFC Security Classification Officer. This report, in its entirety, has been determined to be unclassified.



JAMES C. BLAIR

Director, Structures and Dynamics Laboratory